**Article:**
Dewald, N., Lewington, E.L.M., Livingstone, S.J. et al. (2021) Distribution, characteristics and formation of esker enlargements. Geomorphology, 392. 107919. ISSN: 0169-555X

https://doi.org/10.1016/j.geomorph.2021.107919

# Distribution, Characteristics and Formation of Esker Enlargements

Nico Dewald[a], Emma L.M. Lewington[a], Stephen J. Livingstone[a], Chris D. Clark[a], Robert D. Storrar[b]

[a] *Department of Geography, University of Sheffield, Sheffield, United Kingdom*
[b] *Department for the Natural and Built Environment, Sheffield Hallam University, Sheffield, United Kingdom*

**Abstract**

Eskers are primarily ridges of glaciofluvial sediment deposited in subglacial, englacial and supraglacial conduits. They are typically straight to sinuous features, however, their planform morphology can be highly diverse. Esker enlargements are spatially confined ridge sections that are significantly wider than the trunk ridge (typically 250-400 m) and that reconverge downflow. The enlargements include complex ridge networks or coherent sediment bodies. We mapped >1400 esker enlargements across Fennoscandia and Keewatin, Canada, to investigate their distribution and morphological characteristics. Esker enlargements are less abundant below marine limit, and tend to become more abundant in areas of faster ice retreat. They form local clusters along particular ridges, and can occasionally be traced laterally between adjacent esker systems. Based on morphological observations, we link their formation to roof collapses in subglacial conduits. The distribution of esker enlargements indicates that subglacial conduit collapse became an increasingly significant process during the final stages of deglaciation of both the Scandinavian and Laurentide ice sheets, and may have exerted a positive feedback on ice sheet retreat at land-terminating ice margins.

*Keywords:* esker, esker enlargement, conduit collapse, subglacial hydrology, ice sheet deglaciation

## 1. Introduction

Subglacial meltwater is an important control on the flow dynamics of ice sheets and glaciers. It affects their velocity by opposing the cryostatic pressure, reducing basal drag and initiating local ice-bed decoupling (e.g. Iken and Bindschadler, 1986; Clarke, 2005). However, limited access to the base of glaciers and ice sheets makes subglacial environments challenging to study. An alternative approach to understanding subglacial processes is to study landforms and sediments produced by the flow of ice and meltwater at the bed that have been preserved following ice retreat (Stokes et al., 2015; Greenwood et al., 2016). Landform studies have been facilitated by the availability of high-resolution digital elevation models (DEMs), which now allow us to study their morphology in exceptional detail (Dowling et al., 2013; Chandler et al., 2018).

Eskers are ridges of glaciofluvial material (mostly sand and gravel) typically deposited by water flowing through subglacial conduits (Banerjee and McDonald, 1975; Brennand, 1994, and references therein). They are important indicators of channelised meltwater flow and are thus used to study the structure of subglacial palaeo-drainage systems (c.f. Benn and Evans, 2010; Brennand, 2000; Storrar et al., 2014b). Although eskers are often illustrated as straight to sinuous single-ridges, their along-ridge morphology can vary significantly. Sinuosity (Storrar et al., 2014b), ridge dimensions (Burke et al., 2012b, 2015; Perkins et al., 2016) and number of crests and/or ridges (Price, 1966; Shilts et al., 1987; Perkins et al., 2016; Storrar et al., 2020) are principal planform-characteristics leading to manifold esker configurations.

Variations in esker width are widely reported and exhibit a range of morphologies (Brennand, 1994; Burke et al., 2012b, 2015; Gorrell and Shaw, 1991; Hebrand and Åmark, 1989; Perkins et al., 2016; Shilts et al., 1987). They can be expressed as ridge-scale bulges (approximately 50% wider than trunk ridge; Perkins et al. 2016) denoting subglacial depocentres of dynamically adjusting conduits (Burke et al., 2015) or multi-ridged segments formed by meltwater flow diversion (Shilts et al., 1987; Gorrell and Shaw, 1991; Brennand, 1994; Hooke, 2005; Burke et al., 2012b; Perkins et al., 2016; Storrar et al., 2020).

A variety of mechanisms have been invoked for the formation of multi-ridged esker sections including; 1) subglacial conduit choking forcing meltwater paths to diverge (Shilts et al., 1987; Menzies and Shilts, 1996; Storrar et al., 2015, 2020); 2) subglacial conduit breaching on ascending slopes (Shreve, 1972, 1985); 3) the establishment of a broad zone of minor conduits alongside the main subglacial conduit in response to enhanced water flow (Gorrell and Shaw, 1991; Brennand, 1994); 4) unstable conduit positions on top of previously deposited ridges creating secondary (or tertiary, etc.) eskers alongside the main esker (Hooke, 2005) or; 5) sedimentation within abandoned supraglacial channels with successive shifts in supraglacial stream position generating a series of ridges which are superimposed on one another as the ice ablates (Bennett and Glasser, 1996; Huddart et al., 1999; Bennett et al., 2009).

Complex ridge patterns observed in esker systems on formerly glaciated beds have variously been termed "esker

nets", "anastomosing eskers" or "complex eskers" (Persson, 1974; Shaw et al., 1992; Hooke, 2005; Shaw and Kvill, 2011; Storrar et al., 2015; Johnson et al., 2019; Storrar et al., 2015; Sutinen et al., 2009). Lindström (1993) applied the term "esker enlargement" to describe both single and multi-ridged segments with reconverging downflow stretches that are up to 500% wider than the trunk ridge (Svenonius, 1882; Lindström, 1993). In this study, we use the latter term to refer to significant ridge-widenings that reconverge towards the trunk ridge downflow.

In plan-view, the architecture of esker enlargements comprise both complex ridge networks and coherent sediment bodies with shallow superficial channels (Fig. 1; Lindström 1993). Lindström (1993) studied both the morphology and sedimentology of esker enlargements in northern Sweden and linked their formation to waning subglacial water flow velocities and identified valley geometry, bedrock rises, former bead deposition, drainage confluence, strong melting, stagnant ice and lake drainage as potential causes in connection with ice fracturing and varying sediment discharge. Flodhammar (2011) related the formation of two esker enlargements in southern Sweden to high meltwater discharges over marginal dead ice blocks.

Only a few studies have focussed on esker enlargements and their broader role in the drainage of glaciers and ice sheets (e.g. Svenonius, 1882; Lindström, 1993; Flodhammar, 2011). In this study, we tackle this knowledge gap by mapping esker enlargements across large parts of Fennoscandia and Keewatin (north-central Canada). We then use these data to describe and quantify their morphology and distribution and propose a model for their formation. The implications are then explored in relation to large-scale meltwater drainage, retreat patterns and ice dynamics.

## 2. Regional settings

The Scandinavian Ice Sheet (SIS) covered large parts of northern Europe repeatedly throughout the Quaternary (Batchelor et al., 2019). During the last deglaciation the ice sheet retreated over Fennoscandia from approx. 17 ka to 10 ka BP (Fig. 2A). While the deglaciation of southern Sweden started as early as 17 ka BP, the eastern parts of Finland were exposed considerably later at approx. 13 ka BP (Hughes et al., 2016; Stroeven et al., 2016). During the Younger Dryas cold period (12.7-11.5 ka BP; Lohne et al. 2013), glacial standstills and re-advances formed extensive moraine systems around Fennoscandia and most prominently in southern Finland (Andersen et al., 1995; Lunkka et al., 2020). Retreat following the Younger Dryas cold period was generally faster (Stroeven et al., 2016) and directed towards the Scandes Mountain Range where the ice sheet eventually disintegrated around 10 ka BP (Fig. 2A; Hughes et al. 2016; Stroeven et al. 2016). Records of subglacial meltwater activity such as eskers (Fig. 2A, Boulton et al. 2009; Stroeven et al. 2016), hummock corridors (Peterson and Johnson, 2017; Peterson et al., 2017) and murtoos (Mäkinen et al., 2017; Ojala et al., 2019) have been widely documented. Concurrent with ice sheet retreat, deglaciated coastal areas around the modern Baltic Sea and the Gulf of Bothnia were inundated by water (Björck, 1995; Ojala et al., 2013; Rosentau et al., 2021; Wohlfarth et al., 2008).

Keewatin is located to the west of Hudson Bay in northern Canada (Fig. 2B). During the last glaciation a dome of the former Laurentide Ice Sheet (LIS) was centred over Keewatin and acted as a major ice dispersal centre (Lee et al., 1957; Dyke and Prest, 1987; McMartin and Henderson, 2004). This area records the final stages of deglaciation between approx. 10-7 ka BP (Fig. 2B) in response to increased summer insolation (Carlson et al., 2008, 2009). During ice sheet retreat there were marine incursions in eastern (Tyrrell Sea; Shilts et al. 1987), and northern Keewatin (Prest et al., 1968; Dyke, 2004). There is widespread evidence of subglacial meltwater activity including eskers and meltwater corridors radiating out from the migrating ice divide, directly beneath which they are rare (Shilts et al., 1987; Aylsworth and Shilts, 1989; Storrar et al., 2013, 2014b; Lewington et al., 2020; McMartin et al., 2020). Esker formation here has been linked to increased surface meltwater associated with rapid melting of the LIS towards the end of deglaciation (Storrar et al., 2014a).

## 3. Data and Methods

Our study area includes Norway, Sweden, Finland (Fennoscandia) and parts of Keewatin (Canada). Mapping was carried out from high-resolution (1-2 m) national DEMs in combination with the 2 and 5 m resolution ArcticDEM (Porter et al. 2018; Table 1). We created hillshaded DEMs in ArcMap 10.7 with 45° altitude illumination angles and two contrasting azimuths (45° and 315°) to ensure the detection of elongated azimuth-parallel features (Chandler et al., 2018). Eskers and esker enlargements were mapped manually as line and point layers, respectively, in ArcMap 10.7 and QGIS 3.10. For Keewatin, we used an expanded dataset based on esker ridges mapped by Storrar et al. (2013) (Lewington, 2020). Following Lindström (1993), we define esker enlargements as ridge segments that are significantly wider than the trunk ridge (approx. >300%) and that reconverge downflow (Fig. 3A). Multi-ridged enlargements with fewer than 3 subparallel ridges were excluded from our mapping to avoid the inclusion of minor, multi-ridged sections, e.g. kettle holes (Fig. 1A).

The length and width of all mapped esker enlargements were manually measured to assess their planform morphometry. Length was measured as a straight line from the point of divergence to the (approximated) point of convergence. Width was measured as a straight line perpendicular to the length measurement at the widest part of the enlargement. Where this was not reasonable (e.g. due to bending of the enlargement), width was measured perpendicular to the approximate centreline. Lateral erosion of previously fan-shaped sediment bodies may have resulted in the formation of apparently reconverging features that

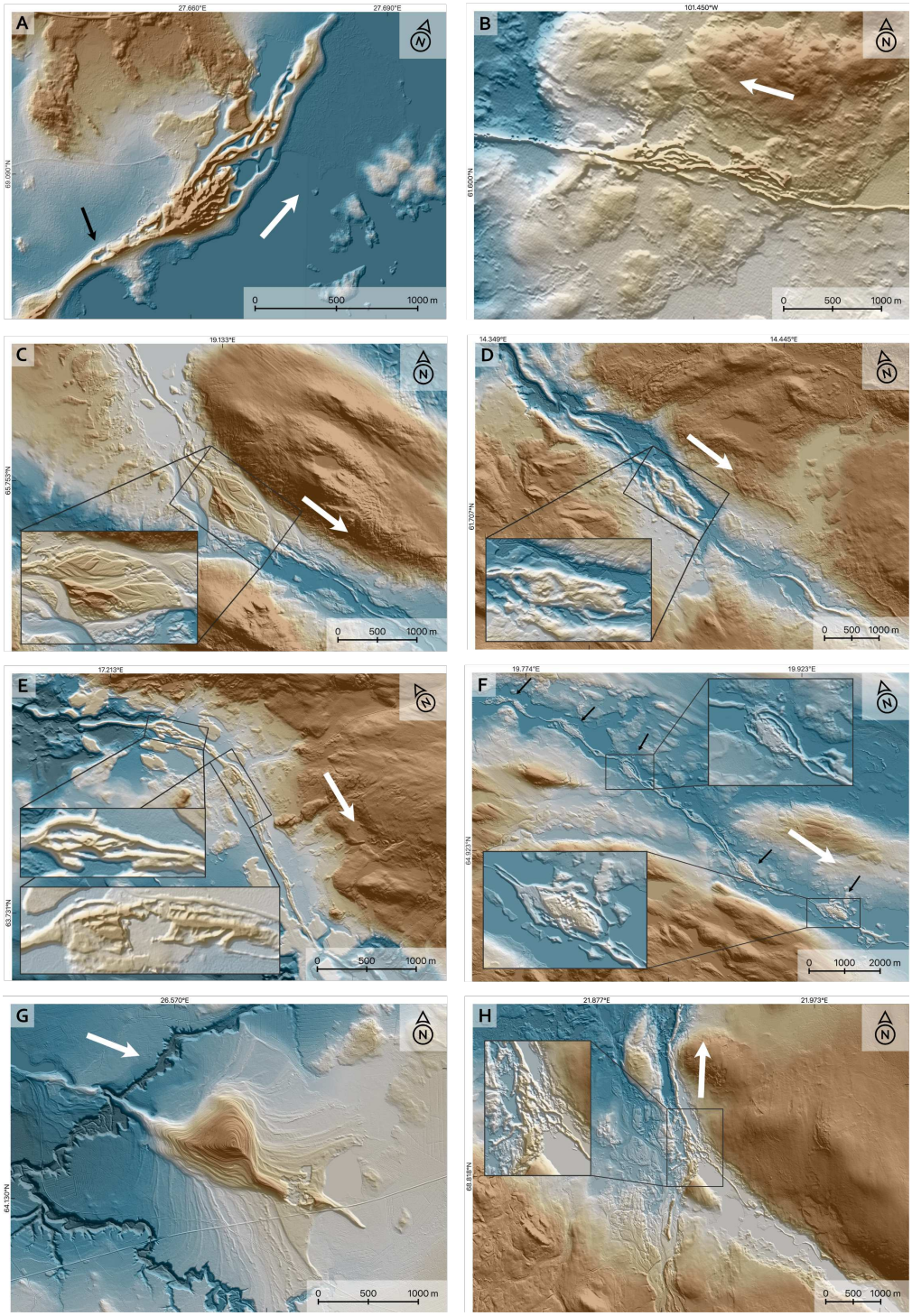


Figure 1: Esker enlargements are prominent widenings of an esker that manifest either as a network of ridges, which diverge and then reconverge downflow, or exist as an elliptical shaped body of sediment. Here we show some diversity of styles of esker enlargements. All panels: brown colours denote higher elevation. White arrows indicate downstream direction. See Fig. 2 for locations. **A**-**B**: Complex esker enlargements comprise a multitude of interrelated ridge crests with varying angles of intersection. Note kettle hole (black arrow in A) and the associated change in ridge crest(s). **C**: Low confidence-enlargement; this looks like a flat-topped esker enlargement but its planform geometry appears to have been modified by erosional channels. **D**: Irregular esker enlargement. **E**: Pair of elongated enlargements. **F**: Cluster along a single ridge. Black arrows point to individual enlargements. **G**: Irregular esker enlargement with superimposed shorelines indicating post-depositional modification. **H**: Esker enlargement at an esker tributary. A, G and H contain data from National Land Survey of Finland Elevation model 2m 11/19. B: ArcticDEM, 5m. C-F: GSD-Höjddata, grid 2+ ©Lantmäteriet.

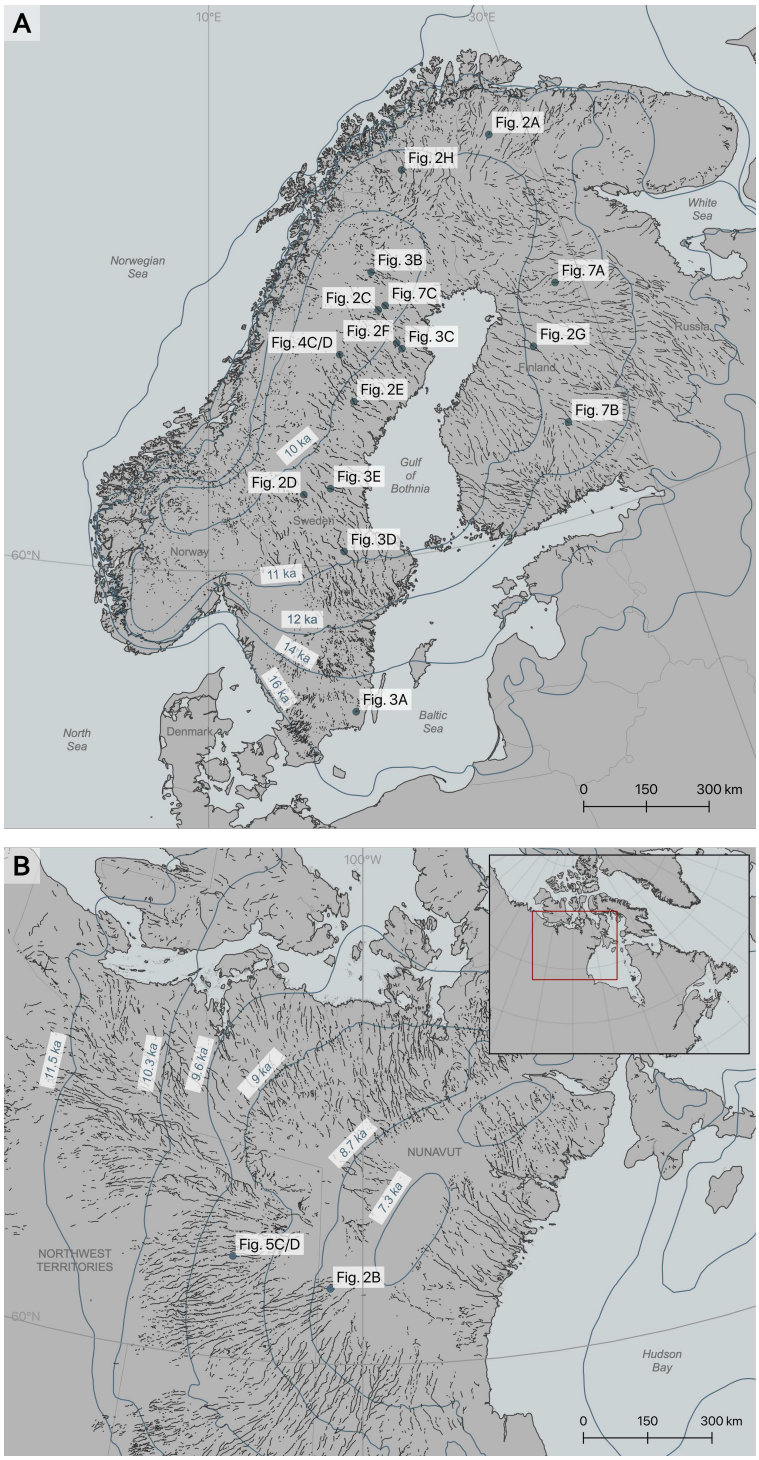


Figure 2: Overview map, figure locations, esker ridges and deglacial chronology for our study areas. **A**: Fennoscandia. Selected ice margin positions from Hughes et al. (2016, most credible). Esker ridges from Stroeven et al. (2016). **B**: Keewatin, Canada. Selected ice margin positions and calibrated radiocarbon dates from Dalton et al. (2020). Esker ridges from Lewington (2020).

Table 1: Data sources

| Country | Data source | Horizontal resolution [m] | Website |
|---|---|---|---|
| Canada | ArcticDEM v7 | 2-5 | https://www.pgc.umn.edu/data/arcticdem |
| Finland | National Land Survey of Finland | 2 | https://www.maanmittauslaitos.fi/en |
| Norway | Kartverket | 1-2 | https://hoydedata.no/LaserInnsyn |
| Sweden | Lantmäteriet | 2 | https://www.lantmateriet.se |

may not be 'real' esker enlargements and are termed 'low confidence-enlargements' (Fig. 1C). To avoid any bias, features with obvious signs of lateral channel cutting and/or that do not transition into esker ridges (i.e. low-confidence enlargements) were excluded from maps and statistics in this paper.

## 4. Results

### *4.1. Distribution*

Esker enlargements occur over large parts of Fennoscandia (Fig. 4A). We mapped 877 features over an approximately 1.1 million km$^2$ area comprising Sweden (n=436), Finland (n=428) and Norway (n=13). Of these, 147 features were classified as low confidence-enlargements, most of which (n=112) are located in Sweden. Sixty-two enlargements were found at esker confluences. Using the total length of mapped eskers (Stroeven et al., 2016) we derive an average frequency of 2.1 esker enlargements per 100 km of esker ridge in our study area. The greatest abundance of esker enlargements occur in central and northern Sweden and eastern Finland (Fig. 4A) while areas inundated by precursors of the Baltic Sea (i.e. below the highest palaeoshoreline;Ojala et al. 2013) show slightly lower counts of esker enlargements (Fig. 4A). The western part of the SIS including Norway and the Scandes mountain range have few eskers (Stroeven et al., 2016) and are largely devoid of enlargements.

Esker enlargements are also common across Keewatin, and unlike in Fennoscandia, they tend to cluster in two areas, rather than be more widespread (Figs. 4A and 5A). We mapped 532 features across an approximately 1 million km$^2$ area, 25 of which were classified as low confidence-enlargements. Twenty-four esker enlargements were recorded at esker tributaries. Using the total length of mapped eskers (Lewington, 2020) we derive an average frequency of 2.1 esker enlargements per 100 km esker ridge in our study area, the same as for Fennoscandia. Esker enlargements are largely absent beneath the former ice sheet divide. The highest density of esker enlargements occurs in the SW of the study area, while they are much rarer in the east and northern sectors (Fig. 5A), which coincide with the highest marine limits (Prest et al., 1968).

The distribution of esker enlargements among esker systems is heterogeneous and they tend to occur in clusters along particular esker systems while adjacent segments are devoid of them (Figs. 4B and 5B; c.f. Lindström 1993). We define a cluster as a group of three or more esker enlargements along a common esker system that are within 10 km of each other (Fig. 1F). Five hundred and twelve esker enlargements (41%) were found to occur within clusters, of which we identify 59 in Fennoscandia and 64 in Keewatin. The mean cluster size (number of esker enlargements) is 4.0 for Fennoscandia and 4.4 for Keewatin. The maximum cluster size found in each study area is 11 (Fig. 6A).

Esker systems hosting esker enlargements are typically less fragmented (Fig. 6B). The median lengths for continuous ridge segments hosting enlargements are 7.3 km for Fennoscandia and 2.9 km for Keewatin (using eskers from Stroeven et al. (2016) and Lewington (2020), respectively). These are considerably higher than the median lengths of all esker ridges in the respective study areas (1.3 km for Fennoscandia and 0.4 km for Keewatin; Fig. 6B). Some esker enlargements seem to have a lateral equivalent on adjacent esker systems less than 20 km apart. We counted 69 such pairs in Fennoscandia and 65 in Keewatin (Fig. 4C,D showing 4 pairs of which one includes a low confidence-enlargement; Fig. 5C,D showing 2 pairs). Examples from two exceptionally close esker systems (<3 km apart) in central Sweden and a confluent system in western Keewatin not only show lateral equivalences but also concomitant changes in the relative size of esker enlargements downflow (Figs. 4C,D and 5C,D).

### *4.2. Morphology*

The planform geometry of esker enlargements typically ranges from circular to elliptic (Figs. 1, 3 and 7). Highly elongated features are also occasionally observed (Fig. 1E), but are less common. Our size measurements comprising both study areas range between ca. 200 m up to >3500 m for length and ca. 100 m up to >1500 m for width (Fig. 8). The median length and width are 870 m and 327 m, respectively, comparable to those obtained by Lindström (1993, median length - 1000 m, median width - 475 m) who analysed 32 esker enlargements in northern Sweden. Elongation ratios (length/width) of esker enlargements in Fennoscandia and Keewatin range between 0.81 and 9.18 with a mean of 2.82 and a standard deviation of 1.08 (median=2.59).

The morphologies of esker enlargements show large variations (Figs. 1, 3 and 7). We identified three main forms

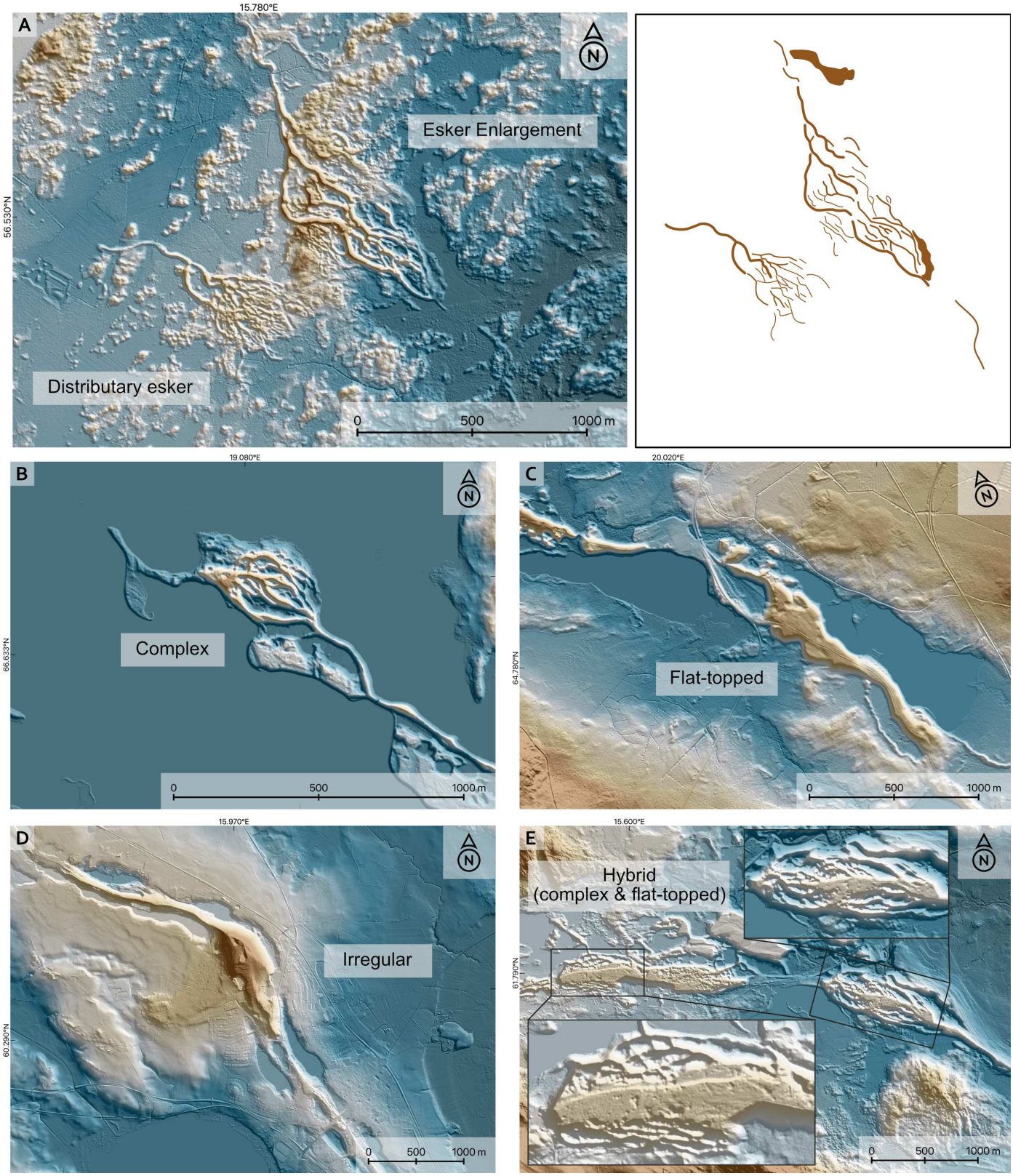


Figure 3: Morphological observations relevant to esker enlargements. **A**: Distinction between distributary eskers (lower left) versus those that we classify as (complex) esker enlargements (upper right). Note that the esker enlargement reconverges towards a single ridge, whereas the distributary system retains a fan-shaped plan-form. Shaded polygons in the right panel denote undefined sediment accumulations. **B**: Complex esker enlargement **C**: Flat-topped esker enlargement **D**: Irregular esker enlargement **E**: Hybrids between complex and flat-topped esker enlargements. Note that flat-topped areas dominate the western feature whereas the eastern feature is dominated by a complex morphology. All panels: brown colours denote higher elevations; GSD-Höjddata, grid 2+ ©Lantmäteriet.

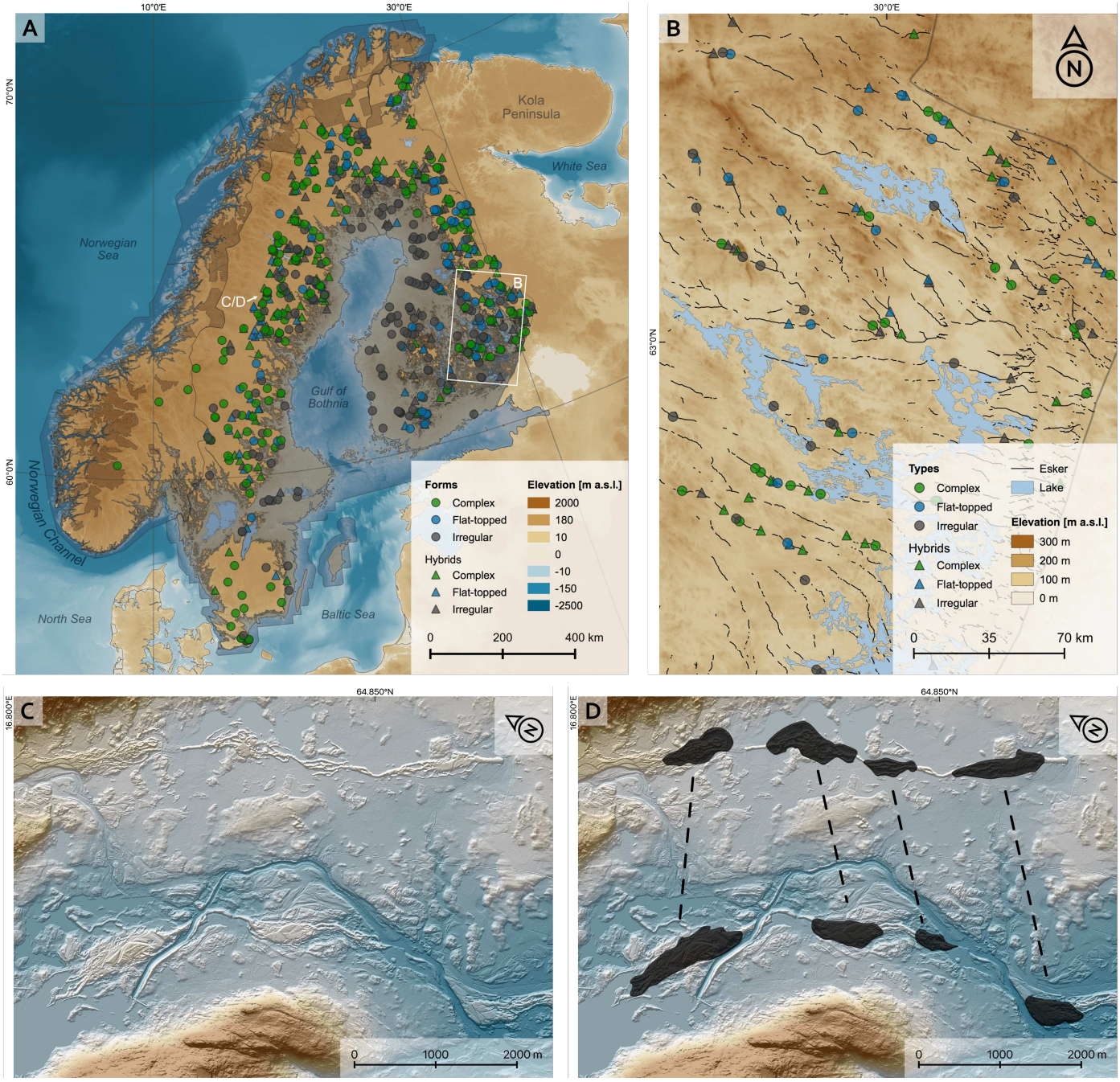


Figure 4: Distribution (A), clustering (B) and lateral equivalences (C/D) of esker enlargements in Fennoscandia. Investigated area is Norway, Sweden and Finland only. Hybrid features (triangles) are coloured according to prevailing morphology (aerially most extensive). Grey in A denotes the area below the highest shoreline. Dark brown polygons in Norway and Finland denote missing elevation data. All panels: brown colours denote higher elevations. **A**: Note relative abundance of features above the highest shoreline and predominance of non-complex morphologies in areas below the highest shoreline. **B**: Note abundance of esker ridges along particular ridges while adjacent ones have only little or no features (see A for location). Grey line indicates the margin of study area. **C**: Two adjacent esker systems in central Sweden (see A for location). **D**: Indication of how approximate size and position of esker enlargements can be linked to features on the adjacent ridge. Elevation basemap data in A and B: GEBCO Compilation Group (2020). C and D: GSD-Höjddata, grid 2+ ©Lantmäteriet.

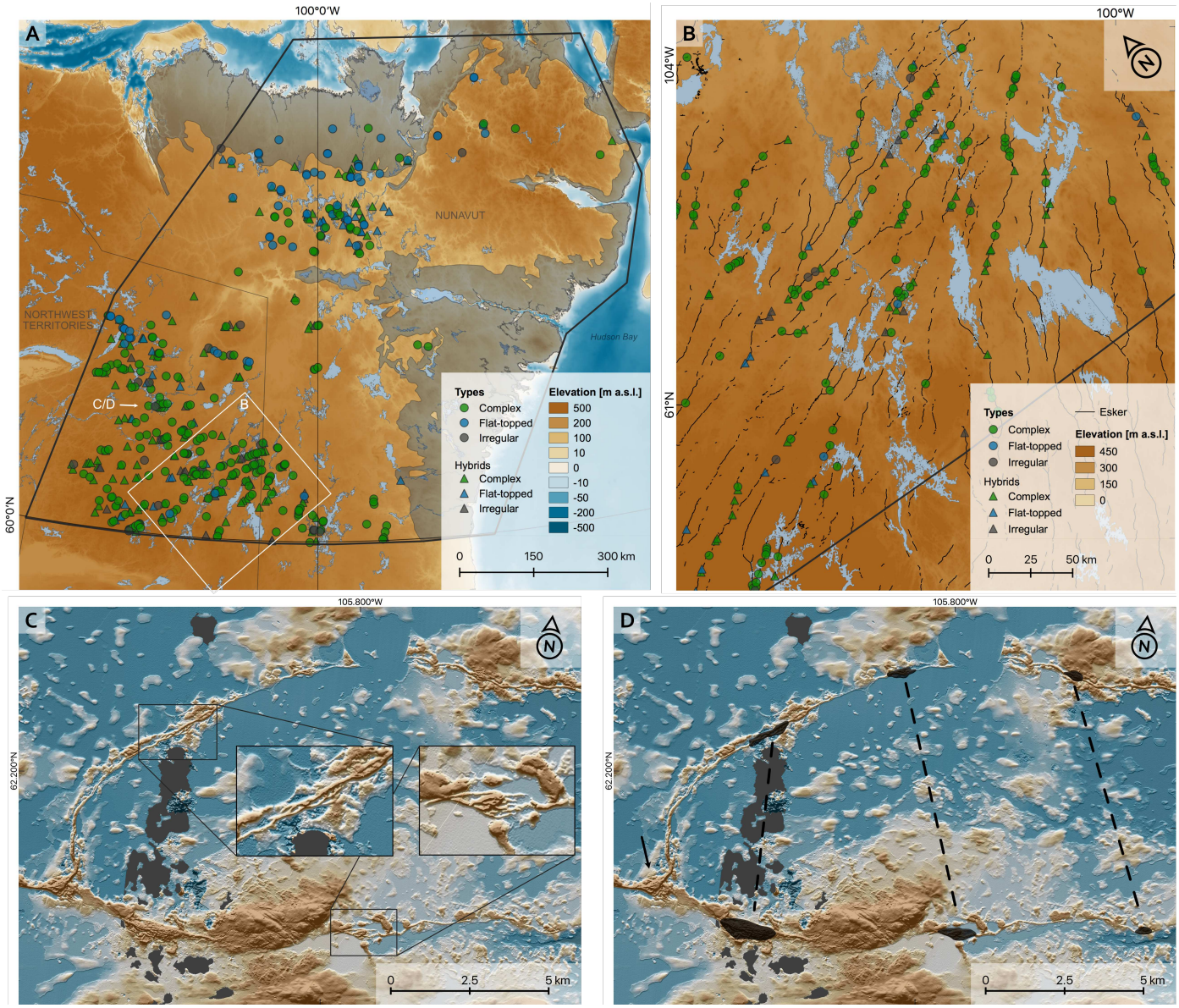


Figure 5: Distribution (A), clustering (B) and lateral equivalences (C/D) of esker enlargements in Keewatin, Canada. Black box in A indicates study area. Hybrid features (triangles) are coloured according to prevailing morphology (aerially most extensive). Grey in A denotes the area below the highest shoreline. Dark grey areas in C and D are missing elevation data. All panels: brown colours denote higher elevations **A**: Note relative abundance of features above highest shoreline. **B**: Note abundance of esker ridges along particular ridges while adjacent ones have only little or no features (see A for location). **C**: Two confluent esker systems in western Keewatin (see A for location). D: Indication of how approximate size and position of esker enlargements can be linked to features on the adjacent ridge. Note esker enlargement at confluence (arrow). Elevation basemap data in A and B: GEBCO Compilation Group (2020). C and D: ArcticDEM, 5 m.

based on their principal morphological architecture (Fig. 3B-E): complex, flat-topped and irregular (see below). Additionally, features comprising combinations of two or more of the aforementioned forms (complex, flat-topped and irregular) are commonly observed and classified according to their dominant (i.e. aerially most extensive) morphological expression. We refer to these as 'hybrids' (Fig. 3E).

There is no clear spatial pattern in the distribution of individual forms of esker enlargements (Figs. 4A and 5A). Exceptions are areas below the highest marine palaeoshoreline, where irregular features are more common, and southern Sweden, where complex enlargements appear to be relatively abundant (Fig. 4A). Similarly, in Keewatin, there is no clear spatial pattern in the distribution of esker enlargement forms (Fig. 5A).

**Complex esker enlargements** are spatially confined ridge networks where individual ridges may superpose each other in places (Figs. 1A,B,H, 3B and 7). Transitions to and from the parent ridge are often smooth but can also be abrupt or show superposition. Their planform geometries are often symmetrical with respect to the trunk ridge. The largest ridges are often found towards the centre and along the flanks while other ridges can be relatively minor (e.g. Fig. 7B). Arcuate ridges are common among this form and may intersect other ridges at angles of up to 90° and usually >45° (e.g. Figs. 1A, 3E and 7B). Small depressions may occur within individual ridges (Fig. 1A). The length of complex esker enlargements in Fennoscandia and Keewatin ranges from 216 m to 2924 m with a median of 798 m (Fig. 8). Widths range between 116 m and 1175 m with a median of 305 m. Their median length and width are the lowest values found among all esker enlargement forms. The vast majority of hybrid features are associated with complex forms and more than half (52%) are dominated by this morphology (Fig. 8).

**Flat-topped esker enlargements** are plateau-like sediment bodies. The transition to and from their parent ridges is often characterised by a relatively continuous change in width towards the trunk esker (e.g. Fig. 1F; Fig. 3C). One or multiple generations of superficial channels are common but not uniformly present (e.g. Figs. 1C and 7C). Small depressions on flat-topped enlargement surfaces create local pockmarked structures (Fig. 7B,C). Flat-topped esker enlargements are among the rarest forms, making up just 11% of all enlargements. However, a number of hybrid features are associated with flat-topped morphologies of which 29% are dominated by flat-topped architectures. Their sizes (excluding hybrids) range from 253 m to 3370 m in length (median: 820 m) and 117 m to 974 m in width (median: 344 m, Fig. 8).

**Irregular esker enlargements** are morphologically coherent features with variable degrees of surface slope and roughness (Figs. 1D,G and 3D). Palaeo-shorelines can be observed on a number of features (Fig. 1G). Due to their commonly irregular shapes the enlargements can be very poorly defined and their identification should thus, in general, be treated with lower confidence relative to other forms. They constitute 16% of all esker enlargements, while 19% of all hybrid features are dominated by irregular surface expressions (Fig. 8). Their lengths range from 264 m to 3035 m with a median of 985 m. Widths range between 94 m and 1318 m with a median of 355 m.

## 5. Discussion

### *5.1. Regional-scale distribution of esker enlargements*

Our study demonstrates the widespread occurrence of esker enlargements in Fennoscandia and Keewatin (Figs. 4A and 5A) and reveals variations in their distribution and morphology. Here, we discuss the distribution of esker enlargements (Figs. 4A and 5A) in relation to what is known regarding rates of ice sheet retreat, changes in subglacial hydrology, and post-glacial erosion.

Esker enlargements can only exist in the presence of eskers. While this relationship does not account for the overall distribution, the paucity of esker enlargements in and around the area of the Scandes mountain range, including Norway can be explained by lower counts and less continuous esker ridges in this area (2A, Stroeven et al. 2016). The frequency and continuity of esker ridges in Sweden and Finland is higher, but with few esker enlargements observed in some areas such as southern Sweden. The paucity of esker enlargements in central Keewatin can be explained by the lack of esker ridges beneath the palaeo-ice divide (Aylsworth and Shilts, 1989; Livingstone et al., 2020; McMartin et al., 2020; Storrar et al., 2013). However, the presence of esker ridges does not always result in esker enlargements; for example there are very few esker enlargements in central Nunavut and areas to the east that were later inundated by the Tyrell Sea (Fig. 5A; Shilts 1986).

On a regional scale, relatively higher densities of esker enlargements coincide spatially with increased ice retreat rates; typically 200-1600 m $yr^{-1}$ following the Younger Dryas in Fennoscandia (Hughes et al., 2016; Stroeven et al., 2016) and 230-540 m $yr^{-1}$ for Keewatin driven by significant surface melting due to early Holocene atmospheric warming (Carlson et al., 2009; Dyke, 2004). In contrast, lower abundances of esker enlargements in southern Sweden roughly correlate with slower retreat rates prior to the Younger Dryas (order of 50-200 m $yr^{-1}$; Stroeven et al. 2016). Similar observations have been documented for Fennoscandian murtoo fields (Ojala et al., 2019). Murtoos are thought to be formed by a sequence of subglacial processes involving increased meltwater fluxes, till and glaciofluvial sediment deposition, and subsequent deformation (Mäkinen et al., 2017; Ojala et al., 2019; Peterson Becher and Johnson, 2021). Their similar arrangement on an ice sheet-scale suggests that esker enlargements, too, share a positive relationship to increased subglacial meltwater fluxes. The reverse of this is also supported by the lack of esker enlargements coincident with mapped esker beads in eastern Keewatin (Lewington, 2020), which have been linked to limited sediment and meltwater fluxes (Livingstone et al., 2020).

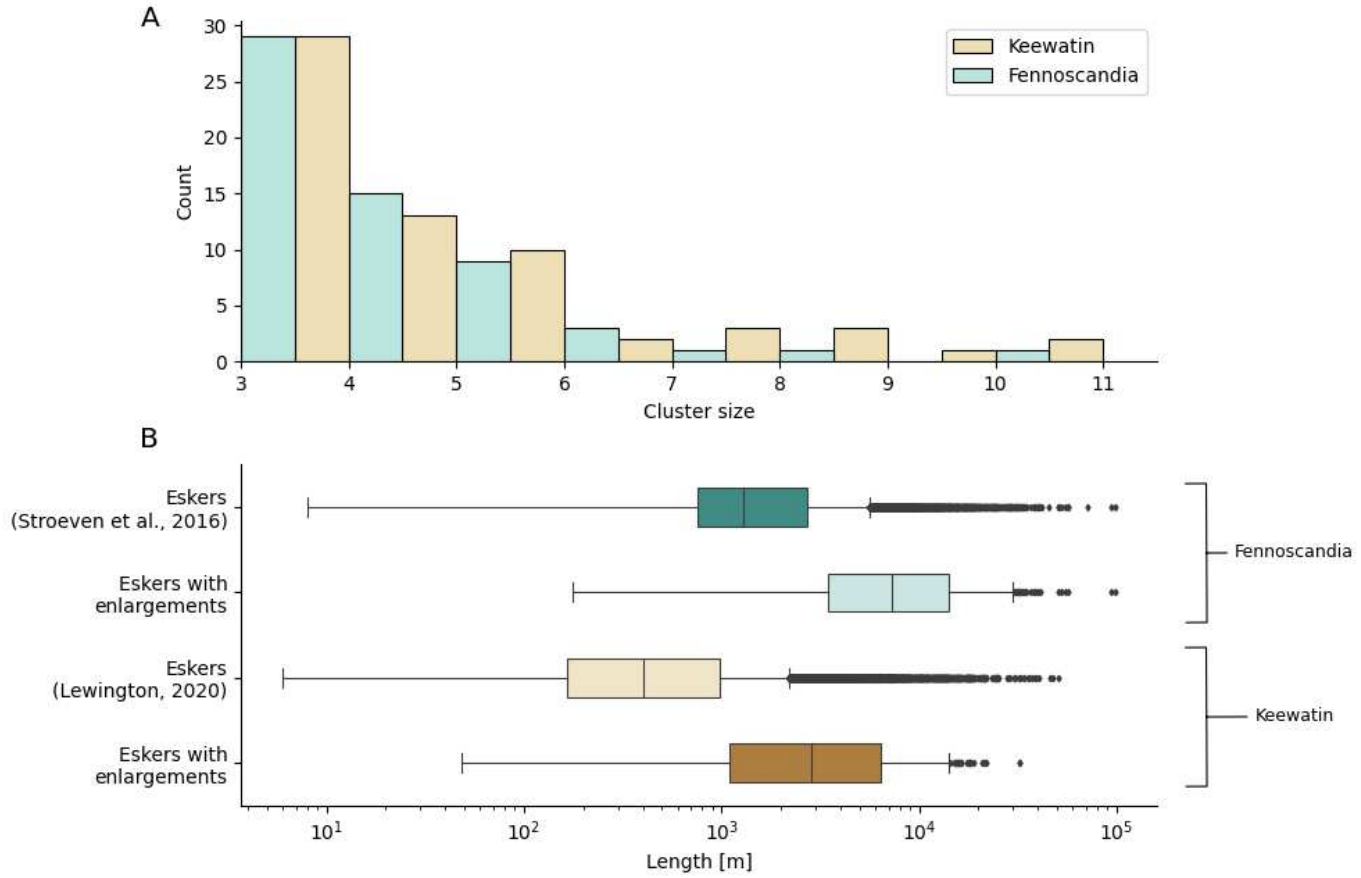


Figure 6: Esker enlargement cluster and esker ridge length statistics. **A**: Distribution of esker enlargement cluster sizes for each study area. A cluster is defined as a group of three or more esker enlargements that occur within 10 km from each other along a common esker system. **B**: Esker ridge lengths for segments hosting enlargements in comparison to all eskers for each study area. Note logarithmic scale and differences in length between eskers hosting esker enlargements and esker ridges in the respective study area.

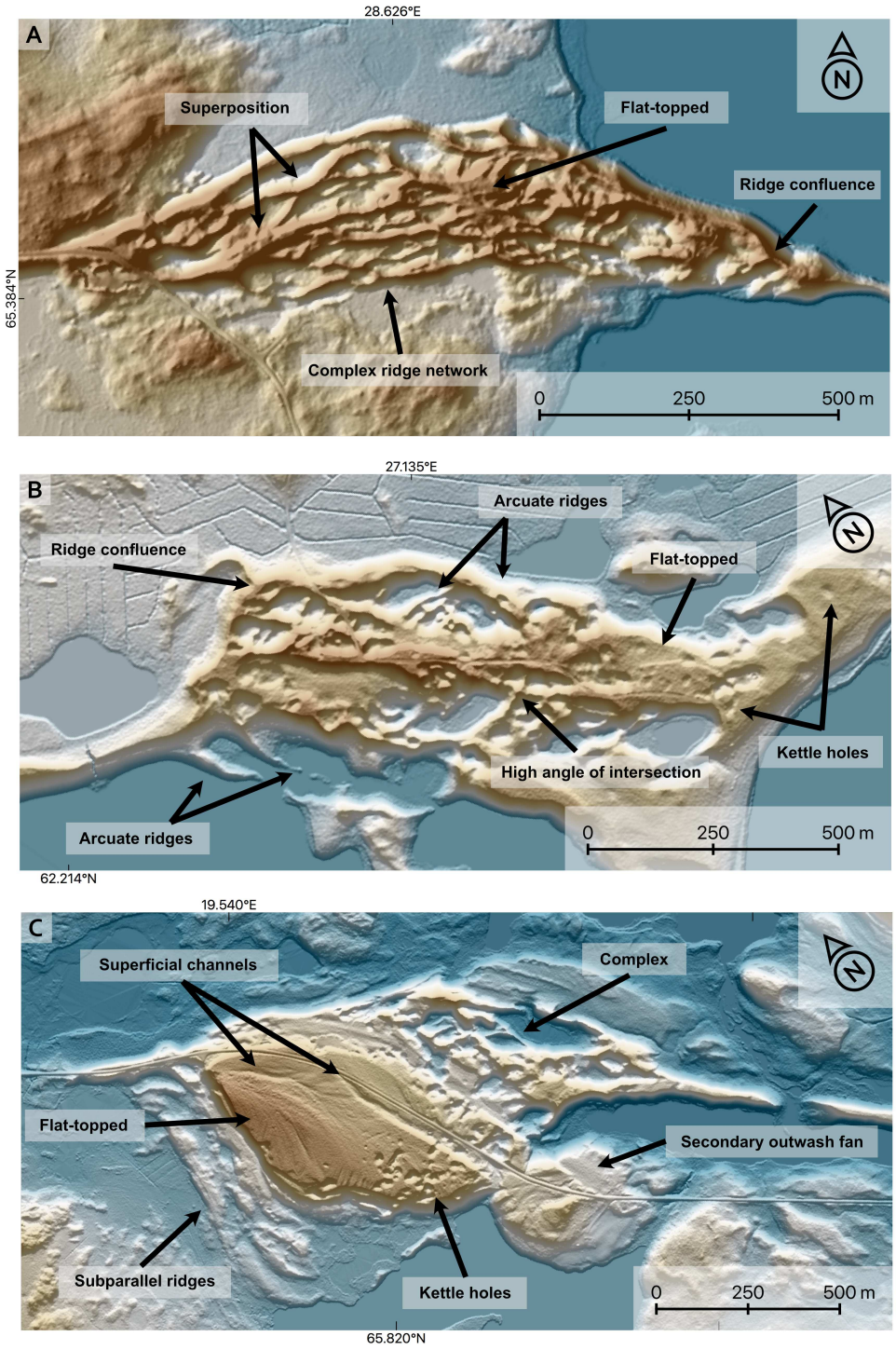


Figure 7: Morphological characteristics of esker enlargements. **A**: Complex esker enlargement with only minor flat-topped parts. Note superposition, ridge confluence and varying size of ridges. **B**: Esker enlargement showing both complex ridge patterns and flat-topped areas and thus classified as 'hybrid' with a dominance in complex morphological architecture. Note the sets of arcuate ridges and their high angles of intersection with other ridges. **C**: Hybrid esker enlargement with a dominance in flat-topped morphology. Note superposition of the plateau and higher elevations of the flat-topped area. All panels: brown colours denote higher elevations. A and B contain data from National Land Survey of Finland Elevation model 2m 11/19. C: GSD-Höjddata, grid 2+ ©Lantmäteriet.

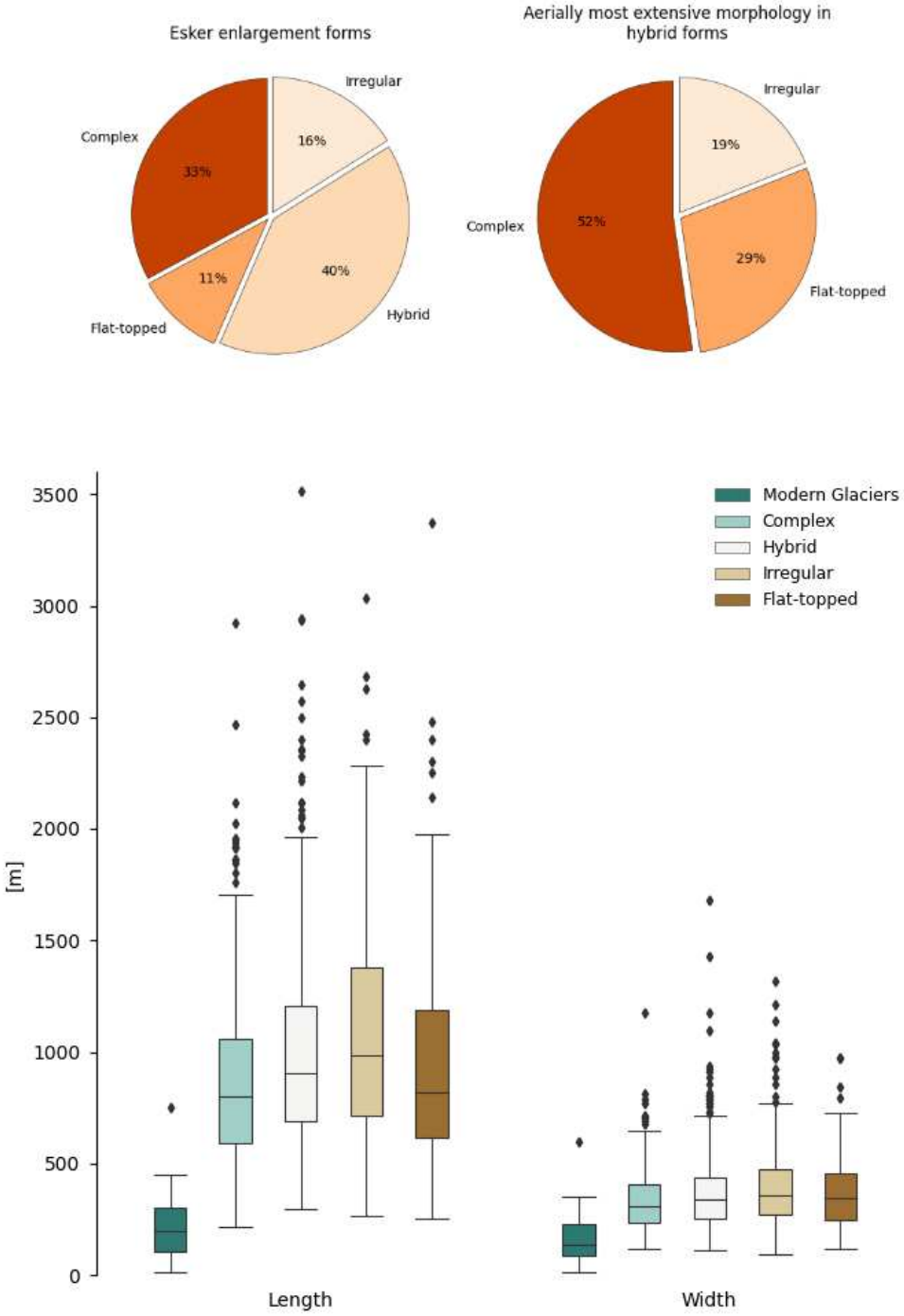


Figure 8: Quantification of esker enlargement forms for both study areas and their comparison to collapse features above subglacial conduits. Note that "predominant morphology" in hybrid features refers to the aerially most extensive morphology. The data for collapse features was gathered from Google Earth imagery. Features were measured across their widest part for length and perpendicular to it for width. Samples (n=17) are derived from Iceland (n=9), Arctic Canada (n=3), Greenland (n=3) and European alpine glaciers (n=2). Note that collapse features mapped on ice caps and glaciers fall within the lower range of the distribution whereas features on Greenland can be much larger (outlier).

The relative abundance of irregular esker enlargement forms below the highest shoreline in Fennoscandia (Figs. 4A and 5A) can be explained by post-depositional reworking and erosion (c.f. Lindström, 1993). This is supported by the frequent observation of superimposed shorelines (Fig. 1G) and the overall larger planform-dimensions of irregular esker enlargements (Fig. 8) that are potentially due to local sediment redistribution caused by wave action. Generally lower feature densities in these areas may at least partially be explained by the effects of post-depositional reworking yielding indistinct, wave-washed landscapes which make (former) enlargements difficult to identify.

The abundance of low confidence-enlargements in Sweden may be attributed to the valley landscape of north and central Sweden. Proglacial meltwater would have been focused down these valleys making it more likely to erode any previously formed enlargements. We are therefore sufficiently confident that the majority of low confidence-enlargements are in fact "real" enlargements, which have been partially eroded. Low confidence-enlargements are rare in Keewatin where generally there is negligible local relief.

### *5.2. Local-scale distribution of esker enlargements*

Chains of esker enlargements along particular esker systems suggest that the individual properties of drainage routes govern the formation of esker enlargements and that these properties were not uniform throughout the subglacial drainage system (likely in both space and time). For example, a chain of enlargements in the downstream part of an esker system, but absent further upstream (cf. Figs. 4B and 5B), indicates a temporal change in drainage and/or glaciological conditions. Furthermore, two adjacent systems, one with and the other without esker enlargements suggests fundamental differences between the two systems (e.g. differing discharges, conduit geometry, bed material, sediment supply, etc...).

The general tendency for esker enlargements to occur along more continuous eskers may be explained by the continuity of the ridges themselves (Fig. 4B; Fig. 5B). The formation of larger, more continuous esker ridges was likely due to enhanced sedimentation rates due to higher discharges and/or sediment supply (Livingstone et al., 2020). This suggests they were major drainage routes that experienced either nearly continuous or episodically above-average meltwater and/or sediment discharges (Storrar et al., 2014b). The relative abundance of esker enlargements along more continuous esker systems suggests a link between discharge/sediment supply and the formation of esker enlargements.

The observation of 134 esker enlargements (approx. 10%) with a lateral equivalent on adjacent esker systems (Figs. 4C,D and 5C,D) suggests a second-order forcing that affected multiple drainage routes at once and in a similar manner, eventually determining the longitudinal position along the esker system. This is most simply explained by the position of the ice margin, indicating a (sub)marginal origin for esker enlargements.

### *5.3. Geomorphology*

In contrast to distributary eskers (Price, 1966; Storrar et al., 2015, 2020), the fundamentally different plan-form geometry of esker enlargements (i.e. enlargement and then re-convergence, Fig. 3A) indicates a spatially confined setting. This characteristic shape of esker enlargements and their immediate association with esker ridges supports a subglacial formation.

Small variations in the planform-dimensions between individual esker enlargement forms and the large number of hybrid features (40%; Fig. 8) suggest a continuum between the different morphologies. This is also supported by the predominance of irregular enlargements in areas of former marine incursion in Fennoscandia, indicating modification by marine processes after initial deposition (see section 4.1). Moreover, flat-topped surfaces of hybrid esker enlargements are typically elevated above ridges indicating that preliminary ridge networks were subsequently covered by sediment (Fig. 7C). It is also interesting to note that 'different' forms of esker enlargements are observed to occur closely along an individual esker ridge and sometimes alternate between different expressions.

### *5.4. A model for the formation of esker enlargements by subglacial conduit collapse*

Complex esker enlargements often show symmetrical planform geometries relative to their parent ridge and are commonly associated with sets of subparallel arcuate ridges (e.g. Figs. 1A, 3B,E and 7B) reminiscent of ice-surface crevasses associated with circular collapse structures (Fig. 9A-D). Circular collapse structures on land-terminating glaciers have been reported from New Zealand (Odell, 1960), North America (Paige, 1956; Morrison, 1958) and Europe (Stocker-Waldhuber et al., 2017; Kellerer-Pirklbauer and Kulmer, 2019; Egli et al., 2021a), and are related to subglacial drainage conduits at stagnating and rapidly receding ice margins (Kellerer-Pirklbauer and Kulmer, 2019; Stocker-Waldhuber et al., 2017). These conduit collapse structures are spatially relatively stable and can be observed at the same position for several years (Stocker-Waldhuber et al., 2017; Kellerer-Pirklbauer and Kulmer, 2019). Circular depressions can also occur above subglacial lakes (e.g. Grímsvötn, Iceland; Björnsson 2003) and on ice shelves ('ice dolines'; Bindschadler et al. 2002). Similarities in the organisation and geometry of complex esker enlargements and crevasse patterns, and their shared link with drainage routeways (eskers) provides the basis for our hypothesis of their submarginal formation.

The location of conduit collapses is likely controlled by the size of the respective conduits and the ice thickness in their vicinity (Stocker-Waldhuber et al., 2017; Kellerer-Pirklbauer and Kulmer, 2019; Egli et al., 2021a). The growth of subglacial conduits is mainly governed by wall melting initiated by the frictional heat of turbulent meltwater flow. Conduit growth is counteracted by creep-closure driven by the thickness of the overlying ice (Röthlisberger, 1972). Subglacial discharge, and thus melting of the


Figure 9: Circular collapse structures and complex esker enlargement. Light blue lines in A-D indicate ice margin **A**: Circular collapse structure on the northeast flank of Breiðamerkurjökull, Iceland. Imagery: Google Earth. Note the subglacial outlet in the bottom right (arrow). **B**: Circular collapse structures on Ferpeclegletscher, European Alps. Imagery: Google Earth. **C**: Circular ponds on Tasman Glacier, New Zealand (white arrows). Note that the ponds nearest the ice margin appear to line up along an inferred subglacial water conduit as indicated by the outlet and river towards the bottom (black arrow). Imagery sourced from https://retrolens.nz and licensed by LINZ CC-BY 3.0 **D**: Incipient collapse structure in Sermilik Fjord on Greenland. Note the circular arrangement of crevasses (black arrows). Imagery: Google Earth E: Complex esker enlargement, Canada (Image: courtesy of Jessey Rice; NRCan Photo Number 2021-076). Note high angle intersections of ridges. Length of feature is approx. 500m.

conduit wall, increases towards the ice margin while the thinner ice reduces the effect of creep closure (Hewitt and Creyts, 2019). Thus, subglacial streams with larger conduit cross-sectional areas close to the ice margin are more likely to collapse (Kellerer-Pirklbauer and Kulmer 2019; Fig. 10). Where the ice surface is sufficiently lowered, the stability of underlying conduits may be disturbed by reductions in ice thickness alone, i.e. without the need for an enlarged conduit (Fig. 10).

In our model, the collapse of subglacial conduit roofs may be triggered by fluctuating meltwater fluxes, local subglacial stream avulsion and/or ice surface thinning (Fig. 11A-B). This may be initiated by either seasonal to multi-annual increases in meltwater runoff or sudden drainage events. Enhanced conduit growth during rising discharge will be followed by a switch to atmospheric pressure (open conduit system) as water flow in the conduit subsequently wanes (Fig. 11C). Due to relatively large cross-sections, which are mostly filled with air, the resulting conduits are prone to collapse. Furthermore, ice-surface lowering due to enhanced surface melting or accelerated flow (Pritchard et al., 2009) may reduce the thickness of ice above conduits leading to weaker ice roofs. Collapse of crevasse-bounded ice that penetrates down to the conduit roof, or even of large ice masses from the unstable conduit roof itself, would then block the water flowing beneath it causing diversions in subglacial stream direction. Occasional choking by sediments deposited in diverging branches causes alternative routes to open which may lead to superimposed ridges. Controlled by the geometry of the collapse structure, the bifurcated streams are reconciled with their original track after they have passed the zone of conduit collapse. Seasonal fluctuations in meltwater discharge deliver sediment which may be deposited between ice blocks and cover some of them entirely (Fig. 11D). Supraglacial streams feeding into the depression may further assist disintegration and could deliver sediment transported from the surface or via melting of debris rich ice (Fig. 9C). As the ice margin retreats past the enlargement, the delivery of sediment via debris-rich ice chunks breaking off the glacier front and melt-out of buried ice may add additional complexity to the resulting ridge pattern. This leads to intricate ridge networks and arcuate patterns common to complex esker enlargements (Figs. 9E and 11F).

Because conduit collapse structures grow or remain active over several years (Stocker-Waldhuber et al., 2017; Kellerer-Pirklbauer and Kulmer, 2019), the processes described above are not necessarily contemporaneous events. Local conduit reorganisation, repeated episodes of sedimentation and reworking of sediments are likely to shape the morphology of esker enlargements over multiple years. Where these processes are accompanied by an increase in sediment supply and/or proglacial lakes affecting the subglacial drainage conditions, formerly deposited structures may become buried leading to flat-topped surfaces (cf. Fig. 7C), particularly along the major drainage axes where ice blocks may melt or be physically removed. Further subaerial runoff across the previously deposited sediment (Fig. 12) would result in superficial channels that are frequently preserved on flat-topped enlargements (Figs. 1C and 7C). Buried chunks of ice may eventually melt and leave kettle-holes leading to complex/flat-topped hybrid patterns (e.g. Fig. 7B). Subsequent re-filling with sediment may result in morphologically undetectable kettle-holes (c.f. Ahokangas and Mäkinen, 2014; Maries et al., 2017).

As ice retreats past the zone of conduit collapse, modern observations suggest that it will form an embayment or ice-walled channel where sediment can easily be trapped (Figs. 9A,B and 12G). Subsequent stream cutting and potential ice melt-out may eventually lead to intricate flat-topped features. These processes are demonstrated at Von Postbreen, Svalbard (Fig. 12G) where ongoing up-stream propagation of an ice-walled corridor, driven by collapse of ice around a subglacial stream, is exposing complex and flat-topped landform morphologies including multiple ponds between individual sediment ridges and ice blocks near the glacier margin. We note that the feature at Von Postbreen is not necessarily analogous to esker enlargements as its geometry and reconvergence is not entirely clear, however we expect processes near the ice margin to be similar for esker enlargements.

Non-fluvial reworking of esker enlargements could result in morphological expressions classified as irregular in our study. This may involve further modification by glacial, aeolian, lacustrine and/or marine processes after their initial exposure. As discussed in section 4.1, the relative abundance of irregular esker enlargements below the highest marine shoreline in Fennoscandia (Figs. 4A and 5A), their frequent association with superimposed palaeo-shorelines (Fig. 1G) and the overall larger planform-dimensions of irregular esker enlargements (Fig. 8) support this idea.

### *5.5. Model correspondence and alternatives*

The idea of conduit-penetrating and collapsing ice blocks diverting subglacial meltwater flow producing anabranching ridge patterns is not new (Shilts et al., 1987; Lindström, 1993; Burke et al., 2012a; Perkins et al., 2016), but a more detailed model for esker enlargement formation has been lacking. Our model provides an explanation for the striking similarities between crevasse patterns associated with conduit collapses on modern ice margins and ridge patterns observed in many complex esker enlargements. The morphological diversity of esker enlargements observed in our mapping can be explained by the interaction of multiple processes including confined sedimentation in collapsing conduit segments, burial and subsequent melt-out of ice blocks, sedimentation in standing water, post-glacial inundation and shoreline migration. Most of these processes likely occur after deposition of an initial complex network of ridges, which is why our model suggests that complex esker enlargements may be a typical precursor to all other forms and combinations thereof. If correct, we would expect to see complex esker ridge networks buried beneath

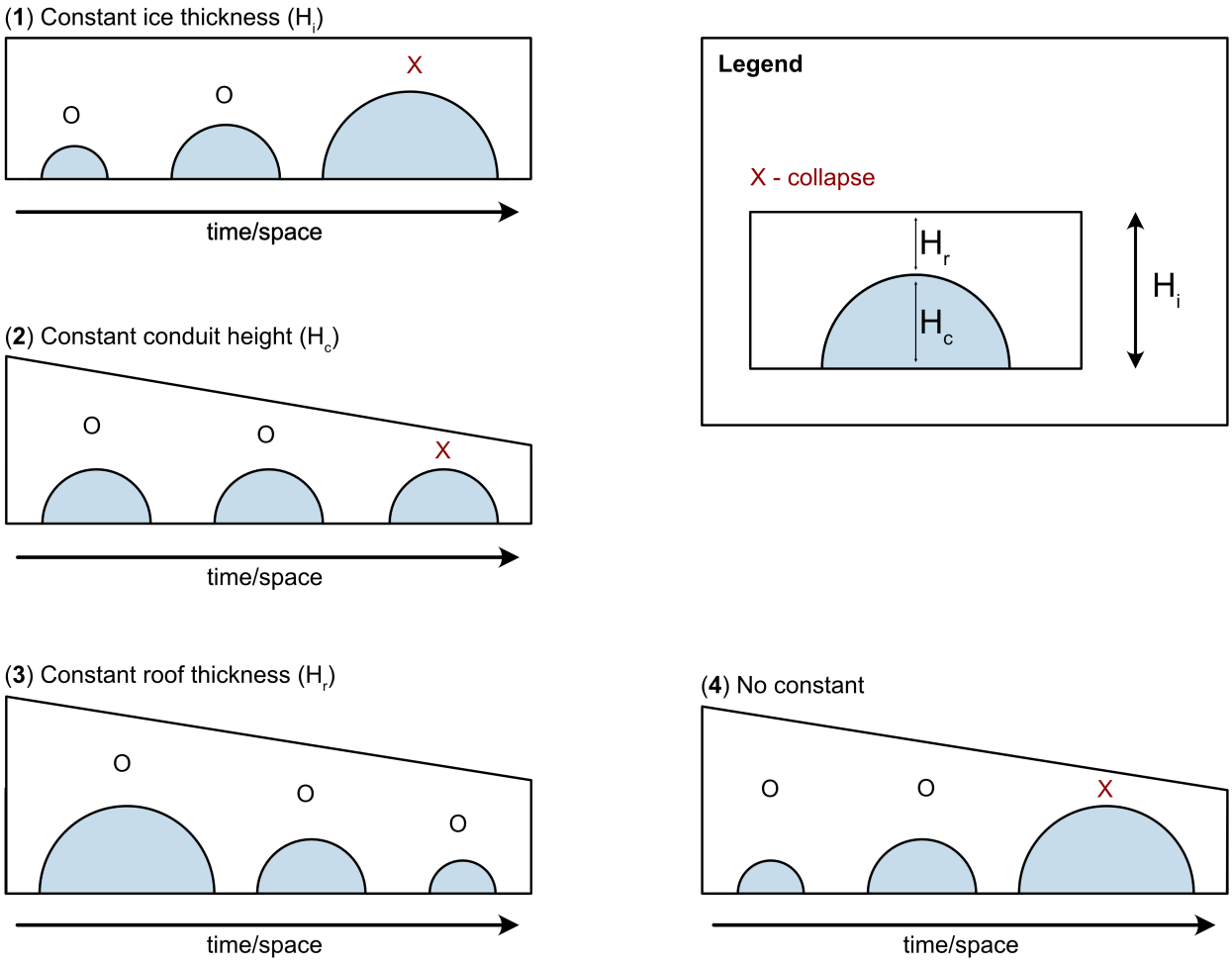


Figure 10: Hypothetical concept for conduit collapses controlled by conduit dimension and ice thickness. Panels 1-4 describe relationships between ice thickness ($H_i$), conduit height ($H_c$) and the resulting thickness above the conduit roof ($H_r = H_i$-$H_c$) for different scenarios. Red crosses mark conditions where conduits are prone to collapse. Note that individual changes displayed in each panel (1-4) may take place in both space and time. This simplified concept describes that conduit collapses are likely to happen where $H_r$ is sufficiently small, suggesting that there may be some kind of threshold (t) where $H_r < t$ produces suitable conditions for conduit collapses. It further depicts the intuitive assumption that both conduit growth (1) and ice surface lowering (2) on their own can lead to conduit collapses but a combination of both (4) is most effective. However, in reality, there are likely other factors such as pre-existing fractures and ice flow velocity influencing the position of collapse structures (Egli et al., 2021b).

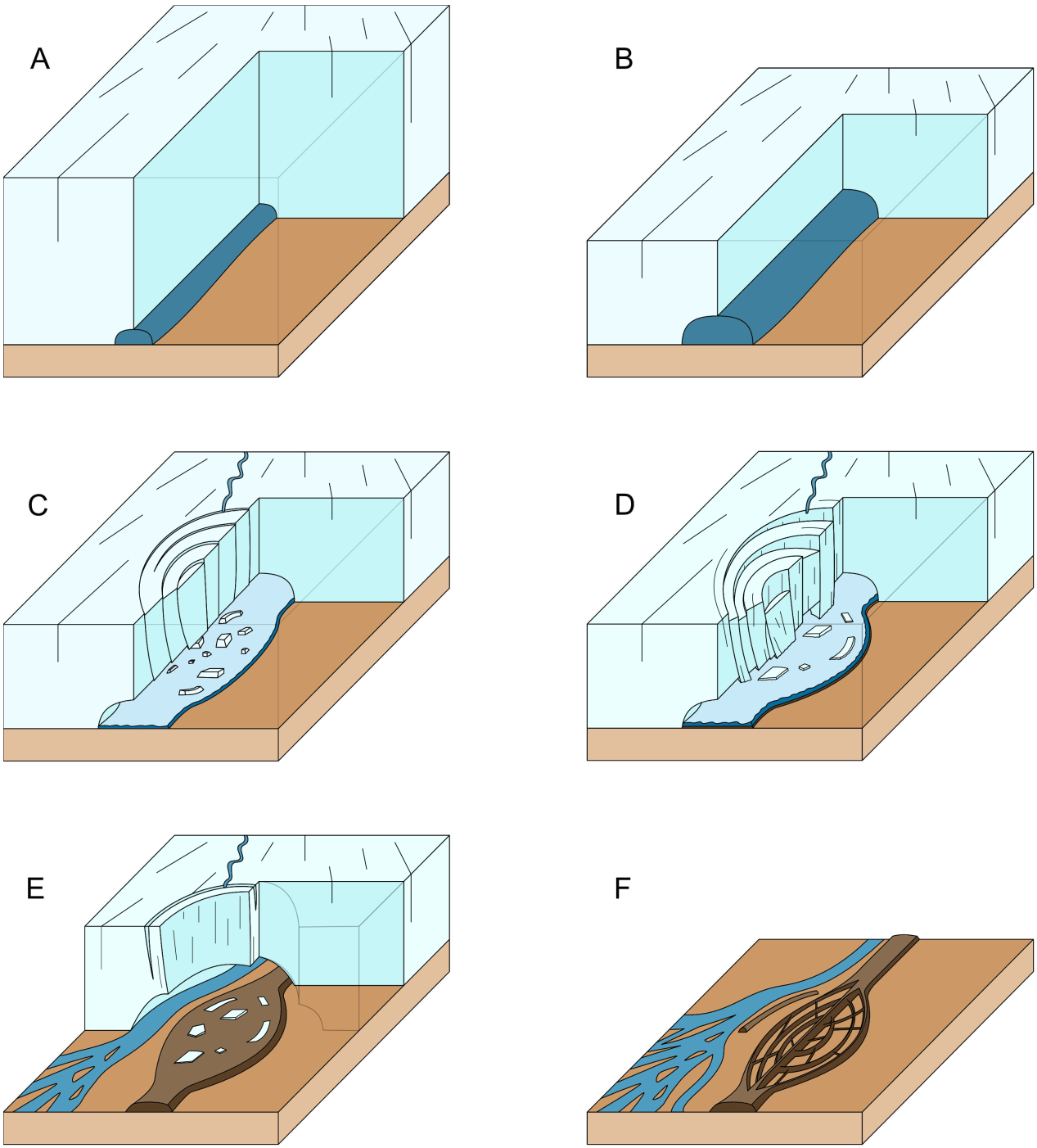


Figure 11: Model for the formation of complex esker enlargements. Note that processes described in this model are not necessarily limited to a single phase and may take place over multiple years. **A**: Small subglacial conduit beneath relatively thick ice evolves into (**B**) a higher-discharge conduit that grows larger once closer to the margin and under thinner ice. **C**: Waning meltwater flow in large conduits depressurises the system causing downward flexing and fracture of the roof. Additional meltwater from the ice surface may feed the circular collapse structure aiding further ablation. **D**: Slightly increasing discharge in the late melt-season causes subglacial water to flow around collapsed ice blocks initiating deposition of sediment in interspaces. **E**: Receding ice margin exposures the sedimentary enlargement with buried arcuate dead ice blocks inherited from the collapse. **F**: Further melt-out and eventual deglaciation leaves an esker enlargement sometimes expressed as a complex network of ridges (illustrated here) and sometimes a massive body of sediment. In this explanation, ridges in the enlargements still record the position of former water flow, as in a main esker thread, but deposited here in a pattern controlled by fractured ice blocks.

other esker enlargement forms. This could be tested by geophysical or sedimentological investigations.

The spatial equivalence between enlargements of adjacent esker systems (Figs. 4C,D and 5C,D) is best explained by a submarginal setting where the ice margin controls the position of enlargements along the respective esker system. Local clusters along esker systems can either be explained by spatio-temporal changes in the hosting subglacial conduits, changes in ice thickness, ice surface slope, ice flow velocity or combinations thereof. Because of the often rather abrupt changes between adjacent esker systems (Figs. 4B and 5B), we suggest that subglacial conduit conditions have a dominant control over the formation of collapse structures. This fits the idea that increasing post-Younger Dryas meltwater discharges caused subglacial conduits to destabilise more often due to increased ice thinning and enhanced conduit growth. The observation of complex esker enlargements at esker confluences (n=86) could also be explained by increased water delivery by converging drainage systems causing conduits to expand leading to subglacial roof collapses. Where ice margins terminated in sufficiently deep water, we also expect conduit collapses to be less likely because the thickness of grounded ice is dependent on water depth and tends to be thicker than terrestrial terminating margins, which results in more stable conduit roofs. This is supported by relatively low numbers of esker enlargements in areas with abundant De Geer moraines below the marine limit (c.f. Bouvier et al., 2015; Ojala, 2016; McMartin et al., 2020). However, topographical variations may lead to shallowly grounded ice that also allows the formation of conduit collapses. Taken together, generally thicker ice at water-terminating ice margins and post-depositional modification may explain the scarcer occurrence and relative abundance of irregular forms of esker enlargements below marine limits in our study areas.

The scales for observed circular conduit collapse structures on modern day glaciers and ice sheets plot at the lower end of the enlargement spectrum (Fig. 8). While there is some overlap in populations, some additional factors may explain the observed deviations: 1) The number of observed collapse features is small (n=17) and may not be representative. 2) We observe significant scale differences between collapse structures on ice sheets and valley glaciers/ice caps (median length 450 m and 170 m respectively; median width 350 m and 104 m, respectively; cf. Fig. 9A,D). The largest collapse feature in our data (750 m long and 600 m wide) was observed on a large outlet glacier on the Greenland Ice Sheet (Fig. 9D), which is experiencing large and rapidly increasing discharges of water and sediment (Overeem et al., 2017). 3) The data for modern collapse features (Fig. 8) was gathered from static images of collapse structures that are likely to have undergone subsequent modifications (Stocker-Waldhuber et al., 2017; Kellerer-Pirklbauer and Kulmer, 2019). A time-series of annual snapshots at Breiðamerkurjökull, Iceland (Fig. 9A-F) confirms this idea and stresses the effect of multi-annual expansion leading to an increased net area affected by the collapse. Accordingly, esker enlargements are expected to be composite features formed by several expansions. Since the expansion of collapse structures is more likely to follow the up or downstream direction of the subglacial conduit, the recorded length of modern collapse structures may not be an accurate measure for comparison against esker enlargements. Width dimensions, which display a closer association between modern collapse structure and esker enlargements (Fig. 8), are likely to have been less affected by subsequent longitudinal expansion and may thus give more reliable results. 4) Eskers developing below modern ice margins are generally smaller than eskers observed on palaeo-ice sheet beds (Banerjee and McDonald, 1975; Brennand, 1994; Jewtuchowicz, 1965; Price, 1966; Storrar et al., 2015), which is likely to be reflected in the size of esker enlargements as well. 5) Lastly, the subglacial area in which sediment gets deposited beneath a collapse structure may be larger than the expression of the respective structure on the ice surface.

Although our model explains a number of observations, we note that there are alternative mechanisms which may have led to the observed structural patterns. Focused delivery of supraglacial meltwater to the bed through moulins can facilitate local diversion of subglacial conduits (Gulley et al., 2012) and vertical intersections with debris-rich ice would provide a further source of sediment to the moulin bottom. If sediment was deposited in moulin-related tunnels to form esker enlargements, the distribution of enlargements would reflect the distribution of moulins. However, this model has difficulties explaining lateral equivalents of enlargements between adjacent esker systems. The complex ridge networks may also reflect subaerial stream avulsion and sedimentation over marginal dead-ice bodies. This model was proposed for a pair of adjacent esker enlargements in southern Sweden (Flodhammar, 2011). However, it struggles to explain the typical reconvergence of esker enlargements and their widely observed sets of arcuate ridges and high intersection angles. Thus, we may expect complex distributary (fan-shaped) esker systems (Storrar et al. 2015; Fig. 3A) to form in proglacial settings or on dead ice.

### *5.6. Implications*

Here, we will discuss the implications of our preferred model (section 5.4), which suggests that esker enlargements and especially clusters of esker enlargements are associated with subglacial conduit collapses along high discharge drainage routes. In assessing the most important drainage routes influencing ice dynamics, it might be that esker size is not the best indicator of conduit size because of the variable effects of sediment availability (Burke et al., 2015). Esker enlargements, however, might be useful indicators of which of the many potential routes were the main, trunk evacuators of subglacial meltwater. This is especially relevant for ice sheet models that incorporate subglacial hydrology where the relatively high resolution of meltwater landform maps (Storrar et al., 2013; Stroeven et al., 2016; Peterson

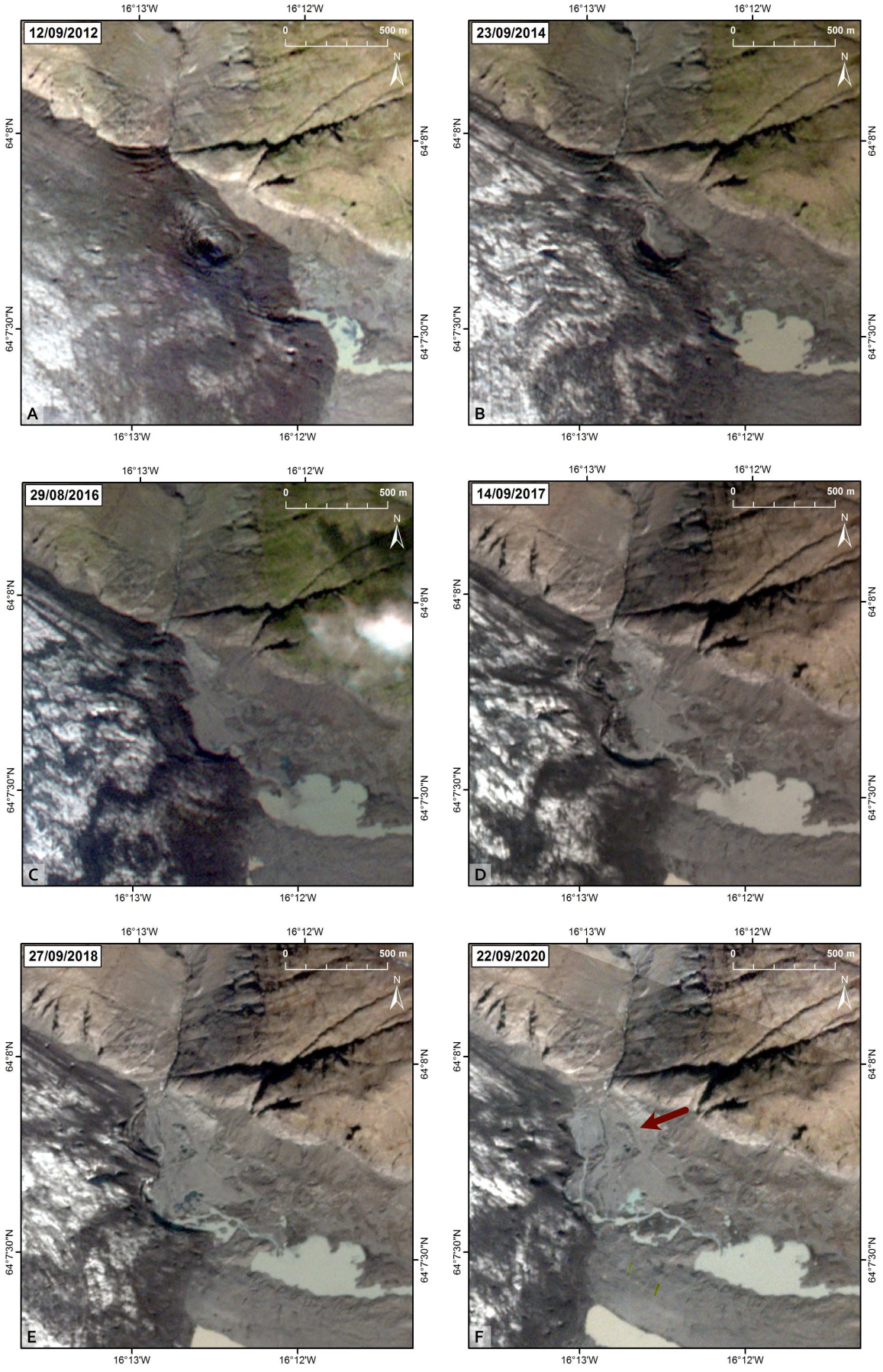
12/09/2012
A
23/09/2014
B
29/08/2016
C
14/09/2017
D
27/09/2018
E
22/09/2020
F
16°13'W
16°12'W
64°8'N
64°7'30'N
0
500 m
N

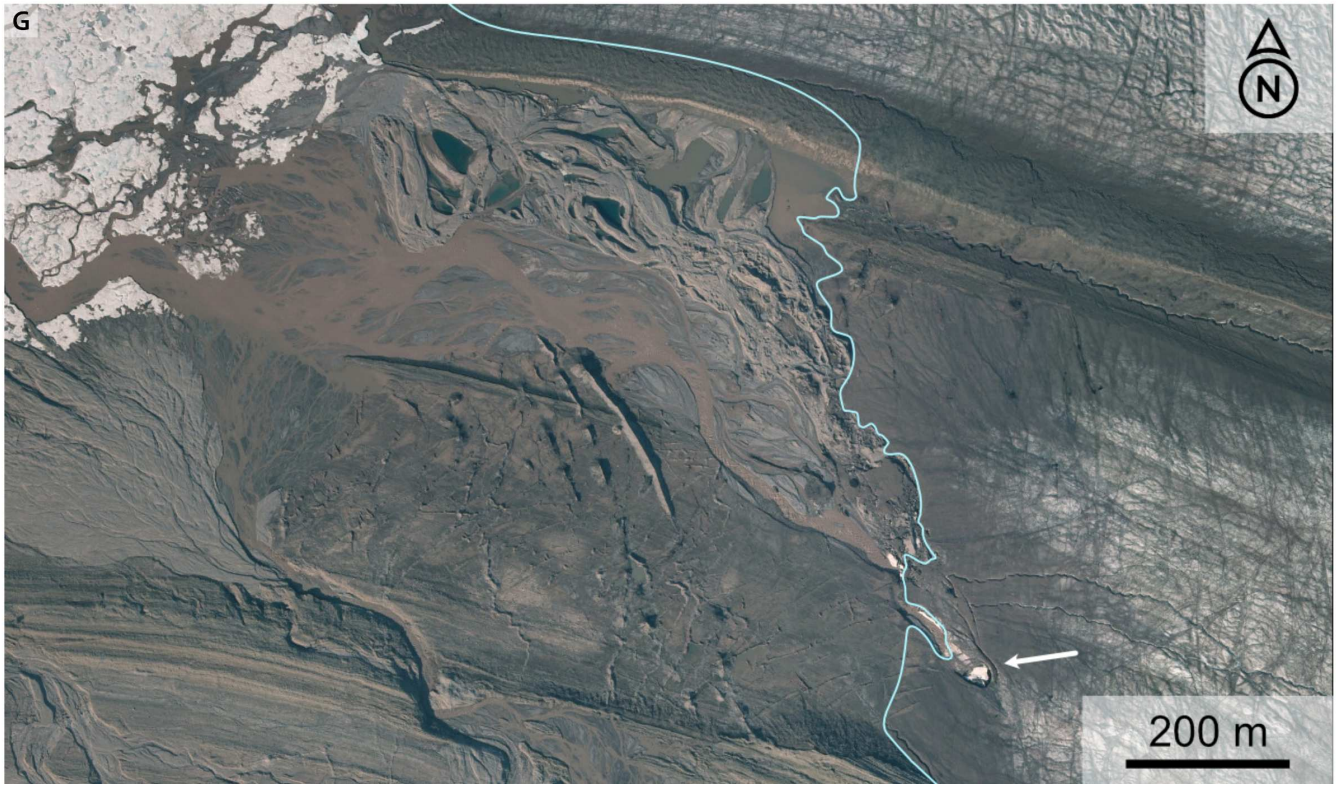


Figure 12: **A-F**: Time series of satellite images showing the evolution of a collapse structure at the margin of Breiðamerkurjökull, Iceland. Note the expansion towards NW in panels D and E yielding an overall larger area affected by the collapse than compared to the initial area in A. Also note minor arcuate ridges emerging in panel E and F (red arrow in F). Imagery © 2021 Planet Labs Inc. **G**: Intricate ridge pattern formed at Von Postbreen, Svalbard. Note collapsing conduit giving way to ice walled channel (white arrow). Note, that this feature is not necessarily analogous to the landforms we envision to be produced by our model. However, it illustrates the association between subglacial conduit collapses and intricate landform morphologies. Light blue line indicates ice margin. Imagery retrieved from https://toposvalbard.npolar.no on 15/03/2021.

et al., 2017; Lewington et al., 2020) cannot be modelled in realistic detail. In such cases, focussing on the major drainage routes would be a reasonable simplification.

Studies on alpine valley glaciers document the disintegration of ice around subglacial conduits by collapse processes (Stocker-Waldhuber et al., 2017; Egli et al., 2021a,b). The distribution of esker enlargements and the formation model that we present here suggests that subglacial conduit collapses occurred widely on palaeo-ice sheets and might thus be a potentially underestimated mechanism influencing ice margin retreat. The regional-scale distribution of esker enlargements further indicates increasingly favourable conditions for their formation towards the later stages of deglaciation in Fennoscandia and Keewatin. We speculate that a similar development could be expected for the Greenland Ice Sheet, which is becoming increasingly land-based due to continuously negative mass balances (Morlighem et al., 2017) and may thus become more susceptible to subglacial conduit collapses in the future. The collapse of subglacial conduits is not widely taken into account when modelling ice dynamics; our research suggests that its importance should be evaluated.

The distribution of esker enlargements may be used to refine rate and timing of ice sheet retreat and aid ice margin reconstructions through their cross flow alignment. This would be particularly useful in areas such as Keewatin where the lack of moraines and remote location have resulted in limited geochronological constraints (Dalton et al., 2020). Furthermore, the relationship between esker enlargements and trunk ridges indicates a genetic link between both features. The sedimentation of esker enlargements is interpreted to occur predominantly submarginally, indicating a submarginal origin for the nearby esker ridges, as well. Since collapse structures are observed to evolve in the late melt season (Stocker-Waldhuber et al., 2017; Kellerer-Pirklbauer and Kulmer, 2019), esker enlargements might also be used to infer more detailed information about the time of esker sedimentation. Lastly, esker ridges have long been known to form tributaries (e.g. Shilts et al., 1987) but the nature of these junctions remains fairly unexplored. Esker enlargements at esker tributary locations are strong indicators for an active confluence of subglacial conduits and may thus be helpful to reconstruct the timing of palaeo-drainage paths.

## 6. Summary and conclusions

We used high-resolution (1-2 m) DEMs to map 877 esker enlargements in Norway, Sweden and Finland and 532 esker enlargements in the Keewatin District of central arctic Canada (2-5 m DEMs). Our study is the first ice sheet-scale documentation of esker enlargements, which demonstrates their widespread occurrence and reveals a wide variety of morphological expressions. Unevenly distributed clusters suggest that their formation was primarily controlled by the conditions imposed by their respective drainage path. Lateral equivalences between adjacent esker systems support a second-order forcing related to processes or conditions in proximity to the ice margin.

Large scale mapping and morphometric analysis of esker enlargements and a comparison to contemporary collapse structures leads us to conclude that esker enlargements are related to subglacial conduit collapses at land-terminating ice margins. Our model explains the variety and distribution of esker enlargements in our data and their widespread occurrence suggests that marginal conduit collapses may have been a recurrent process during deglaciation (especially towards the final stages) in both Fennoscandia and Keewatin.

## 7. Acknowledgements

We wish to thank Jessey M. Rice, Roger C. Paulen and Pascal Egli for valuable discussions about esker enlargements and conduit collapses. We also thank one anonymous reviewer and Rod Smith for numerous comments and useful suggestions that helped us clarify the argument and text. ND was funded by the European Research Council (ERC) project to CDC and this work benefited from the wider PALGLAC team of researchers with funding from the ERC under the European Union's Horizon 2020 research and innovation programme (Grant agreement No. 787263). EL was funded through 'Adapting to the Challenges of a Changing Environment' (ACCE), a NERC-funded doctoral training partnership ACCE DTP (NE/L002450/1). DEMs for Keewatin were provided by the Polar Geospatial Centre under NSF-OPP awards 1043681, 1559691, and 1542736.

## References

Ahokangas, E., Mäkinen, J., 2014. Sedimentology of an ice lobe margin esker with implications for the deglacial dynamics of the Finnish Lake District lobe trunk. Boreas 43, 90–106. URL: https://onlinelibrary.wiley.com/doi/abs/10.1111/bor.12023, doi:10.1111/bor.12023.

Andersen, B.G., Lundqvist, J., Saarnisto, M., 1995. The Younger Dryas margin of the Scandinavian Ice Sheet — An introduction. Quaternary International 28, 145–146. URL: https://www.sciencedirect.com/science/article/pii/104061829500043I, doi:10.1016/1040-6182(95)00043-I.

Aylsworth, J.M., Shilts, W.W., 1989. Bedforms of the Keewatin Ice Sheet, Canada. Sedimentary Geology 62, 407–428. URL: http://www.sciencedirect.com/science/article/pii/0037073889901292, doi:10.1016/0037-0738(89)90129-2.

Banerjee, I., McDonald, B.C., 1975. Nature of Esker Sedimentation Publisher: Special Publications of SEPM.

Batchelor, C.L., Margold, M., Krapp, M., Murton, D.K., Dalton, A.S., Gibbard, P.L., Stokes, C.R., Murton, J.B., Manica, A., 2019. The configuration of Northern Hemisphere ice sheets through the Quaternary. Nature Communications 10, 3713. URL: http://www.nature.com/articles/s41467-019-11601-2, doi:10.1038/s41467-019-11601-2.

Benn, D.I., Evans, D.J.A., 2010. Glaciers and Glaciation. 2. ed., Hodder Education.

Bennett, M., Glasser, N.F., 1996. Glacial Geology: Ice Sheets and Landforms. Wiley, Chichester.

Bennett, M.R., Huddart, D., Thomas, G.S.P., 2009. The Newbigging Esker System, Lanarkshire, Southern Scotland: A Model for Composite Tunnel, Subaqueous Fan and Supraglacial Esker

Sedimentation, in: Hambrey, M.J., Christoffersen, P., Glasser, N.F., Hubbard, B. (Eds.), Glacial Sedimentary Processes and Products. Blackwell Publishing Ltd., Oxford, UK, pp. 177–202. URL: http://doi.wiley.com/10.1002/9781444304435.ch12, doi:10.1002/9781444304435.ch12.

Bindschadler, R., Scambos, T.A., Rott, H., Skvarca, P., Vornberger, P., 2002. Ice dolines on Larsen Ice Shelf, Antarctica. Annals of Glaciology 34, 283–290. URL: https://www.cambridge.org/core/journals/annals-of-glaciology/article/ice-dolines-on-larsen-ice-shelf-antarctica/76E7CA98D7695CB283F07191BFB83665, doi:10.3189/172756402781817996. publisher: Cambridge University Press.

Björck, S., 1995. A review of the history of the Baltic Sea, 13.0-8.0 ka BP. Quaternary International 27, 19–40. URL: http://www.sciencedirect.com/science/article/pii/104061829400057C, doi:10.1016/1040-6182(94)00057-C.

Björnsson, H., 2003. Subglacial lakes and jökulhlaups in Iceland. Global and Planetary Change 35, 255–271. URL: http://www.sciencedirect.com/science/article/pii/S0921818102001303, doi:10.1016/S0921-8181(02)00130-3.

Boulton, G.S., Hagdorn, M., Maillot, P.B., Zatsepin, S., 2009. Drainage beneath ice sheets: groundwater–channel coupling, and the origin of esker systems from former ice sheets. Quaternary Science Reviews 28, 621–638. URL: http://www.sciencedirect.com/science/article/pii/S0277379108002539, doi:10.1016/j.quascirev.2008.05.009.

Bouvier, V., Johnson, M.D., Påsse, T., 2015. Distribution, genesis and annual-origin of De Geer moraines in Sweden: insights revealed by LiDAR. GFF 137, 319–333. URL: https://doi.org/10.1080/11035897.2015.1089933, doi:10.1080/11035897.2015.1089933.

Brennand, T.A., 1994. Macroforms, large bedforms and rhythmic sedimentary sequences in subglacial eskers, south-central Ontario: implications for esker genesis and meltwater regime. Sedimentary Geology 91, 9–55. URL: http://www.sciencedirect.com/science/article/pii/0037073894901228, doi:10.1016/0037-0738(94)90122-8.

Brennand, T.A., 2000. Deglacial meltwater drainage and glaciodynamics: inferences from Laurentide eskers, Canada. Geomorphology 32, 263–293. URL: http://www.sciencedirect.com/science/article/pii/S0169555X99001002, doi:10.1016/S0169-555X(99)00100-2.

Burke, M.J., Brennand, T.A., Perkins, A.J., 2012a. Evolution of the subglacial hydrologic system beneath the rapidly decaying Cordilleran Ice Sheet caused by ice-dammed lake drainage: implications for meltwater-induced ice acceleration. Quaternary Science Reviews 50, 125–140. URL: http://www.sciencedirect.com/science/article/pii/S0277379112002648, doi:10.1016/j.quascirev.2012.07.005.

Burke, M.J., Brennand, T.A., Perkins, A.J., 2012b. Transient subglacial hydrology of a thin ice sheet: insights from the Chasm esker, British Columbia, Canada. Quaternary Science Reviews 58, 30–55. URL: http://www.sciencedirect.com/science/article/pii/S0277379112003393, doi:10.1016/j.quascirev.2012.09.004.

Burke, M.J., Brennand, T.A., Sjogren, D.B., 2015. The role of sediment supply in esker formation and ice tunnel evolution. Quaternary Science Reviews 115, 50–77. URL: http://www.sciencedirect.com/science/article/pii/S0277379115000979, doi:10.1016/j.quascirev.2015.02.017.

Carlson, A.E., Anslow, F.S., Obbink, E.A., LeGrande, A.N., Ullman, D.J., Licciardi, J.M., 2009. Surface-melt driven Laurentide Ice Sheet retreat during the early Holocene. Geophysical Research Letters 36. URL: https://agupubs.onlinelibrary.wiley.com/doi/abs/10.1029/2009GL040948, doi:https://doi.org/10.1029/2009GL040948. _eprint: https://agupubs.onlinelibrary.wiley.com/doi/pdf/10.1029/2009GL040948.

Carlson, A.E., LeGrande, A.N., Oppo, D.W., Came, R.E., Schmidt, G.A., Anslow, F.S., Licciardi, J.M., Obbink, E.A., 2008. Rapid early Holocene deglaciation of the Laurentide ice sheet. Nature Geoscience 1, 620–624. URL: https://www.nature.com/articles/ngeo285, doi:10.1038/ngeo285.

Chandler, B.M., Lovell, H., Boston, C.M., Lukas, S., Barr, I.D., Benediktsson, Í.Ö., Benn, D.I., Clark, C.D., Darvill, C.M., Evans, D.J., Ewertowski, M.W., Loibl, D., Margold, M., Otto, J.C., Roberts, D.H., Stokes, C.R., Storrar, R.D., Stroeven, A.P., 2018. Glacial geomorphological mapping: A review of approaches and frameworks for best practice. Earth-Science Reviews 185, 806–846. URL: https://linkinghub.elsevier.com/retrieve/pii/S0012825217305986, doi:10.1016/j.earscirev.2018.07.015.

Clarke, G.K.C., 2005. Subglacial Processes. Annual Reviews in Earth and Planetary Sciences 33, 247–76.

Dalton, A.S., Margold, M., Stokes, C.R., Tarasov, L., Dyke, A.S., Adams, R.S., Allard, S., Arends, H.E., Atkinson, N., Attig, J.W., Barnett, P.J., Barnett, R.L., Batterson, M., Bernatchez, P., Borns, H.W., Breckenridge, A., Briner, J.P., Brouard, E., Campbell, J.E., Carlson, A.E., Clague, J.J., Curry, B.B., Daigneault, R.A., Dubé-Loubert, H., Easterbrook, D.J., Franzi, D.A., Friedrich, H.G., Funder, S., Gauthier, M.S., Gowan, A.S., Harris, K.L., Hétu, B., Hooyer, T.S., Jennings, C.E., Johnson, M.D., Kehew, A.E., Kelley, S.E., Kerr, D., King, E.L., Kjeldsen, K.K., Knaeble, A.R., Lajeunesse, P., Lakeman, T.R., Lamothe, M., Larson, P., Lavoie, M., Loope, H.M., Lowell, T.V., Lusardi, B.A., Manz, L., McMartin, I., Nixon, F.C., Occhietti, S., Parkhill, M.A., Piper, D.J., Pronk, A.G., Richard, P.J., Ridge, J.C., Ross, M., Roy, M., Seaman, A., Shaw, J., Stea, R.R., Teller, J.T., Thompson, W.B., Thorleifson, L.H., Utting, D.J., Veillette, J.J., Ward, B.C., Weddle, T.K., Wright, H.E., 2020. An updated radiocarbon-based ice margin chronology for the last deglaciation of the North American Ice Sheet Complex. Quaternary Science Reviews 234, 106223. URL: https://linkinghub.elsevier.com/retrieve/pii/S0277379119307619, doi:10.1016/j.quascirev.2020.106223.

Dowling, T.P.F., Alexanderson, H., Möller, P., 2013. The new high-resolution LiDAR digital height model ('Ny Nationell Höjdmodell') and its application to Swedish Quaternary geomorphology. GFF 135, 145–151. URL: https://doi.org/10.1080/11035897.2012.759269, doi:10.1080/11035897.2012.759269.

Dyke, A., Prest, V., 1987. Late Wisconsinan and Holocene History of the Laurentide Ice Sheet. Géographie physique et Quaternaire 41, 237–263. URL: https://www.erudit.org/en/journals/gpq/1900-v1-n1-gpq1945/032681ar/abstract/, doi:10.7202/032681ar. publisher: Les Presses de l'Université de Montréal.

Dyke, A.S., 2004. An outline of North American deglaciation with emphasis on central and northern Canada, in: Ehlers, J., Gibbard, P.L. (Eds.), Developments in Quaternary Sciences. Elsevier. volume 2 of *Quaternary Glaciations-Extent and Chronology*, pp. 373–424. URL: https://www.sciencedirect.com/science/article/pii/S1571086604802094, doi:10.1016/S1571-0866(04)80209-4.

Egli, P.E., Irving, J., Lane, S.N., 2021a. Characterization of subglacial marginal channels using 3-D analysis of high-density ground-penetrating radar data. Journal of Glaciology , 1–14URL: https://www.cambridge.org/core/journals/journal-of-glaciology/article/characterization-of-subglacial-marginal-channels-using-3d-analysis-of-highdensity-groundpenetrating-radar-data/BD475F6E58B32B060441FE9451C48C0B, doi:10.1017/jog.2021.26. publisher: Cambridge University Press.

Egli, P.E., Lane, S.N., Irving, J., Belotti, B., 2021b. Temperate Alpine glacier surface dynamics linked to collapsing subglacial conduits, online.

Flodhammar, I., 2011. Lövestads åsar: En isälvsavlagring bildad vid inlandsisens kant i Weichsels slutskede. Bachelor's thesis. Lund University. Sweden.

GEBCO Compilation Group, 2020. GEBCO 2020 Grid. URL: doi:10.5285/a29c5465-b138-234d-e053-6c86abc040b9.

Gorrell, G., Shaw, J., 1991. Deposition in an esker, bead and fan complex, Lanark, Ontario, Canada. Sedimentary Geology 72, 285–314. URL: http://www.sciencedirect.com/science/article/pii/0037073891900167, doi:10.1016/0037-0738(91)90016-7.

Greenwood, S.L., Clason, C.C., Helanow, C., Margold, M., 2016. Theoretical, contemporary observational and palaeo-perspectives on ice sheet hydrology: Processes and products. Earth-Science Reviews 155, 1–27. URL: http://www.sciencedirect.com/science/article/pii/

S0012825216300095, doi:10.1016/j.earscirev.2016.01.010.

Gulley, J.D., Grabiec, M., Martin, J.B., Jania, J., Catania, G., Glowacki, P., 2012. The effect of discrete recharge by moulins and heterogeneity in flow-path efficiency at glacier beds on subglacial hydrology. Journal of Glaciology 58, 926–940. URL: https://www.cambridge.org/core/journals/journal-of-glaciology/article/effect-of-discrete-recharge-by-moulins-and-heterogeneity-in-flowpath-efficiency-at-glacier-beds-on-subglacial-hydrology/9734138C4BFC1AE1CF9128B241E60992, doi:10.3189/2012JoG11J189. publisher: Cambridge University Press.

Hebrand, M., Åmark, M., 1989. Esker formation and glacier dynamics in eastern Skane and adjacent areas, southern Sweden. Boreas 18, 67–81. doi:10.1111/j.1502-3885.1989.tb00372.x.

Hewitt, I.J., Creyts, T.T., 2019. A model for the formation of eskers. Geophysical Research Letters 46, 6673–6680. URL: https://agupubs.onlinelibrary.wiley.com/doi/abs/10.1029/2019GL082304, doi:10.1029/2019GL082304.

Hooke, R.L., 2005. Principles of glacier mechanics. Cambridge University Press, Cambridge, UK; New York. URL: http://search.ebscohost.com/login.aspx?direct=true&scope=site&db=nlebk&AN=132255. oCLC: 1105435616.

Huddart, D., Bennett, M.R., Glasser, N.F., 1999. Morphology and sedimentology of a high-arctic esker system: Vegbreen, Svalbard. Boreas 28, 253–273. URL: https://onlinelibrary.wiley.com/doi/abs/10.1111/j.1502-3885.1999.tb00219.x, doi:10.1111/j.1502-3885.1999.tb00219.x.

Hughes, A.L.C., Gyllencreutz, R., Lohne, Ø.S., Mangerud, J., Svendsen, J.I., 2016. The last Eurasian ice sheets - a chronological database and time-slice reconstruction, DATED-1. Boreas 45, 1–45. URL: http://doi.wiley.com/10.1111/bor.12142, doi:10.1111/bor.12142.

Iken, A., Bindschadler, R.A., 1986. Combined measurements of Subglacial Water Pressure and Surface Velocity of Findelengletscher, Switzerland: Conclusions about Drainage System and Sliding Mechanism. Journal of Glaciology 32, 101–119. URL: https://www.cambridge.org/core/journals/journal-of-glaciology/article/combined-measurements-of-subglacial-water-pressure-and-surface-velocity-of-findelengletscher-switzerland-conclusions-about-drainage-system-and-sliding-mechanism/D13B018DF875401A113B477C1885CAB2, doi:10.3189/S0022143000006936.

Jewtuchowicz, S., 1965. Description of Eskers and Kames in Gåshamnöyra and on Bungebreen, South of Hornsund, Vestspitsbergen. Journal of Glaciology 5, 719–725. URL: https://www.cambridge.org/core/journals/journal-of-glaciology/article/description-of-eskers-and-kames-in-gashamnoyra-and-on-bungebreen-south-of-hornsund-vestspitsbergen/3E24478AF144D2DB70163AB37B806261, doi:10.3189/S0022143000018712. publisher: Cambridge University Press.

Johnson, M.D., Wedel, P.O., Benediktsson, Í., Lenninger, A., 2019. Younger Dryas glaciomarine sedimentation, push-moraine formation and ice-margin behavior in the Middle Swedish end-moraine zone west of Billingen, central Sweden. Quaternary Science Reviews 224, 105913. URL: https://linkinghub.elsevier.com/retrieve/pii/S0277379119303142, doi:10.1016/j.quascirev.2019.105913.

Kellerer-Pirklbauer, A., Kulmer, B., 2019. The evolution of brittle and ductile structures at the surface of a partly debris-covered, rapidly thinning and slowly moving glacier in 1998–2012 (Pasterze Glacier, Austria). Earth Surface Processes and Landforms 44, 1034–1049. URL: https://onlinelibrary.wiley.com/doi/abs/10.1002/esp.4552, doi:https://doi.org/10.1002/esp.4552. _eprint: https://onlinelibrary.wiley.com/doi/pdf/10.1002/esp.4552.

Lee, H., Craig, B., Fyles, J., 1957. Keewatin ice divide. Geological Society of America Bulletin 68, 1760–1761.

Lewington, E.L.M., 2020. New insights into subglacial meltwater drainage pathways from the ArcticDEM. Ph.D.. University of Sheffield. Sheffield.

Lewington, E.L.M., Livingstone, S.J., Clark, C.D., Sole, A.J., Storrar, R.D., 2020. A model for interaction between conduits and surrounding hydraulically connected distributed drainage based on geomorphological evidence from Keewatin, Canada. The Cryosphere 14, 2949–2976. URL: https://tc.copernicus.org/articles/14/2949/2020/, doi:https://doi.org/10.5194/tc-14-2949-2020. publisher: Copernicus GmbH.

Lindström, E., 1993. Esker Enlargements in Northern Sweden. Geografiska Annaler. Series A, Physical Geography 75, 95–110. URL: http://www.jstor.org/stable/521028, doi:10.2307/521028. publisher: [Wiley, Swedish Society for Anthropology and Geography].

Livingstone, S.J., Lewington, E.L.M., Clark, C.D., Storrar, R.D., Sole, A.J., McMartin, I., Dewald, N., Ng, F., 2020. A quasi-annual record of time-transgressive esker formation: implications for ice sheet reconstruction and subglacial hydrology URL: https://www.the-cryosphere-discuss.net/tc-2019-273/tc-2019-273.pdf, doi:10.5194/tc-2019-273.

Lohne, Ø.S., Mangerud, J., Birks, H.H., 2013. Precise 14C ages of the Vedde and Saksunarvatn ashes and the Younger Dryas boundaries from western Norway and their comparison with the Greenland Ice Core (GICC05) chronology. Journal of Quaternary Science 28, 490–500. URL: https://onlinelibrary.wiley.com/doi/abs/10.1002/jqs.2640, doi:https://doi.org/10.1002/jqs.2640. _eprint: https://onlinelibrary.wiley.com/doi/pdf/10.1002/jqs.2640.

Lunkka, J.P., Palmu, J.P., Seppänen, A., 2020. Deglaciation dynamics of the Scandinavian Ice Sheet in the Salpausselkä zone, southern Finland. Boreas n/a. URL: https://onlinelibrary.wiley.com/doi/abs/10.1111/bor.12502, doi:https://doi.org/10.1111/bor.12502. _eprint: https://onlinelibrary.wiley.com/doi/pdf/10.1111/bor.12502.

Mäkinen, J., Kajuutti, K., Palmu, J.P., Ojala, A., Ahokangas, E., 2017. Triangular-shaped landforms reveal subglacial drainage routes in SW Finland. Quaternary Science Reviews 164, 37–53. URL: http://www.sciencedirect.com/science/article/pii/S0277379116307181, doi:10.1016/j.quascirev.2017.03.024.

Maries, G., Ahokangas, E., Mäkinen, J., Pasanen, A., Malehmir, A., 2017. Interlobate esker architecture and related hydrogeological features derived from a combination of high-resolution reflection seismics and refraction tomography, Virttaankangas, southwest Finland. Hydrogeology Journal 25, 829–845. URL: http://link.springer.com/10.1007/s10040-016-1513-9, doi:10.1007/s10040-016-1513-9.

McMartin, I., Godbout, P.M., Campbell, J.E., Tremblay, T., Behnia, P., 2020. A new map of glacigenic features and glacial landsystems in central mainland Nunavut, Canada. Boreas URL: https://onlinelibrary.wiley.com/doi/abs/10.1111/bor.12479, doi:https://doi.org/10.1111/bor.12479. _eprint: https://onlinelibrary.wiley.com/doi/pdf/10.1111/bor.12479.

McMartin, I., Henderson, P., 2004. Evidence from Keewatin (Central Nunavut) for Paleo-Ice Divide Migration. Géographie physique et Quaternaire 58, 163–186. URL: http://www.erudit.org/en/journals/gpq/2004-v58-n2-3-gpq1285/013137ar/abstract/, doi:https://doi.org/10.7202/013137ar.

Menzies, J., Shilts, W.W., 1996. Subglacial Environments, in: Past Glacial Environments: Sediments, Forms and Techniques. Butterworth-Heinemann, Oxford, UK.

Morlighem, M., Williams, C.N., Rignot, E., An, L., Arndt, J.E., Bamber, J.L., Catania, G., Chauché, N., Dowdeswell, J.A., Dorschel, B., Fenty, I., Hogan, K., Howat, I., Hubbard, A., Jakobsson, M., Jordan, T.M., Kjeldsen, K.K., Millan, R., Mayer, L., Mouginot, J., Noël, B.P.Y., O'Cofaigh, C., Palmer, S., Rysgaard, S., Seroussi, H., Siegert, M.J., Slabon, P., Straneo, F., van den Broeke, M.R., Weinrebe, W., Wood, M., Zinglersen, K.B., 2017. BedMachine v3: Complete Bed Topography and Ocean Bathymetry Mapping of Greenland From Multibeam Echo Sounding Combined With Mass Conservation. Geophysical Research Letters 44, 11,051–11,061. URL: https://agupubs.onlinelibrary.wiley.com/doi/abs/10.1002/2017GL074954, doi:https://doi.org/10.1002/2017GL074954. _eprint: https://agupubs.onlinelibrary.wiley.com/doi/pdf/10.1002/2017GL074954.

Morrison, A., 1958. Circular crevasses, lakeless shores and rotating glaciers of the Homathko Snowfield. Canadian Alpine Journal 41, 86–88.

Odell, N.E., 1960. The Mountains and Glaciers of New Zealand. Journal of Glaciology 3, 739–744. URL: https://www.cambridge.org/core/journals/journal-of-glaciology/article/mountains-and-glaciers-of-new-zealand/3A45B69D9C63EC17590C74A5CFCB40FF, doi:10.3189/S0022143000018049. publisher: Cambridge University Press.

Ojala, A., Palmu, J.P., Åberg, A., Åberg, S., Virkki, H., 2013. Development of an ancient shoreline database to reconstruct the Litorina Sea maximum extension and the highest shoreline of the Baltic Sea basin in Finland. Bulletin of the Geological Society of Finland 85, 127–144. URL: https://www.geologinenseura.fi/sites/geologinenseura.fi/files/bulletin_vol85_2_2013_ojala.pdf, doi:10.17741/bgsf/85.2.002.

Ojala, A.E.K., 2016. Appearance of De Geer moraines in southern and western Finland — Implications for reconstructing glacier retreat dynamics. Geomorphology 255, 16–25. URL: http://www.sciencedirect.com/science/article/pii/S0169555X15302257, doi:10.1016/j.geomorph.2015.12.005.

Ojala, A.E.K., Peterson, G., Mäkinen, J., Johnson, M.D., Kajuutti, K., Palmu, J.P., Ahokangas, E., Öhrling, C., 2019. Ice-sheet scale distribution and morphometry of triangular-shaped hummocks (murtoos): a subglacial landform produced during rapid retreat of the Scandinavian Ice Sheet. Annals of Glaciology , 1–12URL: https://www.cambridge.org/core/journals/annals-of-glaciology/article/icesheet-scale-distribution-and-morphometry-of-triangularshaped-hummocks-murtoos-a-subglacial-landform-produced-during-rapid-retreat-of-the-scandinavian-ice-sheet/929F95AA35351DCB6F2597F090C5F8F3, doi:10.1017/aog.2019.34.

Overeem, I., Hudson, B.D., Syvitski, J.P.M., Mikkelsen, A.B., Hasholt, B., van den Broeke, M.R., Noël, B.P.Y., Morlighem, M., 2017. Substantial export of suspended sediment to the global oceans from glacial erosion in Greenland. Nature Geoscience 10, 859–863. URL: https://www.nature.com/articles/ngeo3046, doi:10.1038/ngeo3046.

Paige, R.A., 1956. Subglacial Stoping or Block Caving: A Type of Glacier Ablation. Journal of Glaciology 2, 727–729. URL: https://www.cambridge.org/core/journals/journal-of-glaciology/article/subglacial-stoping-or-block-caving-a-type-of-glacier-ablation/439D34D8C61EEF4E003E48143130A039, doi:10.3189/S0022143000024977. publisher: Cambridge University Press.

Perkins, A.J., Brennand, T.A., Burke, M.J., 2016. Towards a morphogenetic classification of eskers: Implications for modelling ice sheet hydrology. Quaternary Science Reviews 134, 19–38. URL: https://linkinghub.elsevier.com/retrieve/pii/S0277379115301967, doi:10.1016/j.quascirev.2015.12.015.

Persson, T., 1974. Eskers, plateaux, terraces and other glaciofluvial forms in the southern and central parts of the South-Swedish Highlands. Geologiska Föreningen i Stockholm Förhandlingar 96, 411–419. URL: https://www.tandfonline.com/doi/full/10.1080/11035897409454295, doi:10.1080/11035897409454295.

Peterson, G., Johnson, M.D., 2017. Hummock corridors in the south-central sector of the Fennoscandian ice sheet, morphometry and pattern. Earth Surface Processes and Landforms 43, 919–929. URL: https://onlinelibrary.wiley.com/doi/abs/10.1002/esp.4294, doi:10.1002/esp.4294.

Peterson, G., Johnson, M.D., Smith, C.A., 2017. Glacial geomorphology of the south Swedish uplands – focus on the spatial distribution of hummock tracts. Journal of Maps 13, 534–544. URL: https://doi.org/10.1080/17445647.2017.1336121, doi:10.1080/17445647.2017.1336121.

Peterson Becher, G., Johnson, M.D., 2021. Sedimentology and internal structure of murtoos - V-shaped landforms indicative of a dynamic subglacial hydrological system. Geomorphology 380, 107644. URL: https://www.sciencedirect.com/science/article/pii/S0169555X21000520, doi:10.1016/j.geomorph.2021.107644.

Porter, C., Morin, P., Howat, I., Noh, M.J., Bates, B., Peterman, K., Keesey, S., Schlenk, M., Gardiner, J., Tomko, K., Willis, M., Kelleher, C., Cloutier, M., Husby, E., Foga, S., Nakamura, H., Platson, M., Wethington, Jr., M., Williamson, C., Bauer, G., Enos, J., Arnold, G., Kramer, W., Becker, P., Doshi, A., D'Souza, C., Cummens, P., Laurier, F., Bojesen, M., 2018. ArcticDEM. URL: https://doi.org/10.7910/DVN/OHHUKH, doi:10.7910/DVN/OHHUKH.

Prest, V., Grant, D., Rampton, V., 1968. Glacial Map of Canada.

Price, R.J., 1966. Eskers near the Casement Glacier, Alaska. Geografiska Annaler. Series A, Physical Geography 48, 111–125. URL: https://www.jstor.org/stable/520521, doi:10.2307/520521.

Pritchard, H.D., Arthern, R.J., Vaughan, D.G., Edwards, L.A., 2009. Extensive dynamic thinning on the margins of the Greenland and Antarctic ice sheets. Nature 461, 971–975. URL: https://www.nature.com/articles/nature08471, doi:10.1038/nature08471.

Rosentau, A., Klemann, V., Bennike, O., Steffen, H., Wehr, J., Latinović, M., Bagge, M., Ojala, A., Berglund, M., Becher, G.P., Schoning, K., Hansson, A., Nielsen, L., Clemmensen, L.B., Hede, M.U., Kroon, A., Pejrup, M., Sander, L., Stattegger, K., Schwarzer, K., Lampe, R., Lampe, M., Uścinowicz, S., Bitinas, A., Grudzinska, I., Vassiljev, J., Nirgi, T., Kublitskiy, Y., Subetto, D., 2021. A Holocene relative sea-level database for the Baltic Sea. Quaternary Science Reviews 266, 107071. URL: https://www.sciencedirect.com/science/article/pii/S027737912100278X, doi:10.1016/j.quascirev.2021.107071.

Röthlisberger, H., 1972. Water Pressure in Intra- and Subglacial Channels. Journal of Glaciology 11, 177–203. URL: https://www.cambridge.org/core/journals/journal-of-glaciology/article/water-pressure-in-intra-and-subglacial-channels/63F384A0C25D8CAD2928ABB06D812291, doi:10.3189/S0022143000022188.

Shaw, J., Kargel, J., Strom, R., 1992. Terrestrial Subglacial Landforms as Analogs for Martian Landscapes. URL: http://adsabs.harvard.edu/pdf/1992LPI....23.1273S.

Shaw, J., Kvill, D., 2011. A glaciofluvial origin for drumlins of the Livingstone Lake area, Saskatchewan. Canadian Journal of Earth Sciences URL: https://cdnsciencepub.com/doi/abs/10.1139/e84-150, doi:10.1139/e84-150. publisher: NRC Research Press Ottawa, Canada.

Shilts, W., Aylsworth, J., C.Kaszycki, Klassen, R., 1987. Canadian Shield, in: Geomorphic systems in North America. doi:10.1130/DNAG-CENT-v2.119. journal Abbreviation: Geomorphic systems in North America.

Shilts, W.W., 1986. Chapter 4 Glaciation of the Hudson Bay Region, in: Martini, I.P. (Ed.), Elsevier Oceanography Series. Elsevier. volume 44 of *Canadian Inland Seas*, pp. 55–78. URL: https://www.sciencedirect.com/science/article/pii/S0422989408708973, doi:10.1016/S0422-9894(08)70897-3.

Shreve, R.L., 1972. Movement of Water in Glaciers. Journal of Glaciology 11, 205–214. URL: https://www.cambridge.org/core/journals/journal-of-glaciology/article/movement-of-water-in-glaciers/68CF63EE098E16BE0072489E0BBC16CB, doi:10.3189/S002214300002219X.

Shreve, R.L., 1985. Esker characteristics in terms of glacier physics, Katahdin esker system, Maine. GSA Bulletin 96, 639–646. URL: https://pubs.geoscienceworld.org/gsa/gsabulletin/article-abstract/96/5/639/186670/esker-characteristics-in-terms-of-glacier-physics, doi:10.1130/0016-7606(1985)96<639:ECITOG>2.0.CO;2.

Stocker-Waldhuber, M., Fischer, A., Keller, L., Morche, D., Kuhn, M., 2017. Funnel-shaped surface depressions — Indicator or accelerant of rapid glacier disintegration? A case study in the Tyrolean Alps. Geomorphology 287, 58–72. URL: http://www.sciencedirect.com/science/article/pii/S0169555X16310583, doi:10.1016/j.geomorph.2016.11.006.

Stokes, C.R., Tarasov, L., Blomdin, R., Cronin, T.M., Fisher, T.G., Gyllencreutz, R., Hättestrand, C., Heyman, J., Hindmarsh, R.C.A., Hughes, A.L.C., Jakobsson, M., Kirchner, N., Livingstone, S.J., Margold, M., Murton, J.B., Noormets, R., Peltier, W.R., Peteet, D.M., Piper, D.J.W., Preusser, F., Renssen, H., Roberts, D.H., Roche, D.M., Saint-Ange, F., Stroeven, A.P., Teller, J.T., 2015. On the reconstruction of palaeo-ice sheets: Recent advances and future challenges. Quaternary Science Reviews 125, 15–49. URL: http://www.sciencedirect.com/science/article/

pii/S027737911530055X, doi:10.1016/j.quascirev.2015.07.016.

Storrar, R.D., Evans, D.J.A., Stokes, C.R., Ewertowski, M., 2015. Controls on the location, morphology and evolution of complex esker systems at decadal timescales, Breiðamerkurjökull, southeast Iceland. Earth Surface Processes and Landforms 40, 1421–1438. URL: https://onlinelibrary.wiley.com/doi/full/10.1002/esp.3725, doi:10.1002/esp.3725.

Storrar, R.D., Ewertowski, M., Tomczyk, A.M., Barr, I.D., Livingstone, S.J., Ruffell, A., Stoker, B.J., Evans, D.J.A., 2020. Equifinality and preservation potential of complex eskers. Boreas 49, 211–231. URL: https://onlinelibrary.wiley.com/doi/abs/10.1111/bor.12414, doi:10.1111/bor.12414. _eprint: https://onlinelibrary.wiley.com/doi/pdf/10.1111/bor.12414.

Storrar, R.D., Stokes, C.R., Evans, D.J.A., 2013. A map of large Canadian eskers from Landsat satellite imagery. Journal of Maps 9, 456–473. URL: https://doi.org/10.1080/17445647.2013.815591, doi:10.1080/17445647.2013.815591.

Storrar, R.D., Stokes, C.R., Evans, D.J.A., 2014a. Increased channelization of subglacial drainage during deglaciation of the Laurentide Ice Sheet. Geology 42, 239–242. URL: https://pubs.geoscienceworld.org/gsa/geology/article/42/3/239/131524/increased-channelization-of-subglacial-drainage, doi:10.1130/G35092.1.

Storrar, R.D., Stokes, C.R., Evans, D.J.A., 2014b. Morphometry and pattern of a large sample (>20,000) of Canadian eskers and implications for subglacial drainage beneath ice sheets. Quaternary Science Reviews 105, 1–25. URL: http://www.sciencedirect.com/science/article/pii/S0277379114003618, doi:10.1016/j.quascirev.2014.09.013.

Stroeven, A.P., Hättestrand, C., Kleman, J., Heyman, J., Fabel, D., Fredin, O., Goodfellow, B.W., Harbor, J.M., Jansen, J.D., Olsen, L., Caffee, M.W., Fink, D., Lundqvist, J., Rosqvist, G.C., Strömberg, B., Jansson, K.N., 2016. Deglaciation of Fennoscandia. Quaternary Science Reviews 147, 91–121. URL: http://www.sciencedirect.com/science/article/pii/S0277379115301141, doi:10.1016/j.quascirev.2015.09.016.

Sutinen, R., Piekkari, M., Middleton, M., 2009. Glacial geomorphology in Utsjoki, Finnish Lapland proposes Younger Dryas fault-instability. Global and Planetary Change 69, 16–28. URL: https://www.sciencedirect.com/science/article/pii/S0921818109001179, doi:10.1016/j.gloplacha.2009.07.002.

Svenonius, F., 1882. En åsbilning vid Hornavans sydöstra ända. Geologiska Föreningen i Stockholm Förhandlingar 6, 75–85. URL: https://www.tandfonline.com/doi/full/10.1080/11035898209455533, doi:10.1080/11035898209455533.

Wohlfarth, B., Björck, S., Funder, S., Houmark-Nielsen, M., Ingólfsson, Ó., Lunkka, J.P., Mangerud, J., Saarnisto, M., Vorren, a.T., 2008. Quaternary of Norden. Episodes Journal of International Geoscience 31, 73–81. URL: https://www.episodes.org/journal/view.html?doi=10.18814/epiiugs/2008/v31i1/011, doi:10.18814/epiiugs/2008/v31i1/011. publisher: International Union of Geological Sciences.